Electronic Supplementary Information

Immobilization engineering – How to design advanced sol-gel system for biocatalysis?

Diána Weiser, Flóra Nagy, Gergely Bánóczi, Márk Oláh, Attila Farkas, András Szilágyi, Krisztina László, Ákos Gellért, György Marosi, Sándor Kemény, László Poppe

Table of contents

Materials and enzymes

1.1. Materials

Racemic 1-phenylethan-1-ol (*rac*-**1a**), racemic octan-2-ol (*rac*-**1b**), racemic 1-phenylethan-1-amine (*rac*-**3a**), racemic heptan-2-amine (*rac*-**3b**), sodium fluoride (NaF), polyethylene glycol 1000 (PEG 1000), tetraethoxysilane (TEOS), phenyltriethoxysilane (PTEOS), *n*-octyl-triethoxysilane (OTEOS), dimethyldiethoxysilane (DMDEOS), 2-propanol (IPA), sodium phosphate monobasic, disodium phosphate heptahydrate, vinyl acetate, sodium chloroacetate, sodium, triethylbenzylammonium chloride, p-toluenesulfonic acid, ethyl acetate, magnesium sulfate, Triton X-100, *n*-hexane, acetone, ethanol, methyl *t*-butyl ether (MTBE), water-free toluene and dimethyl-sulfoxyde (DMSO) were commercial products of Alfa-Aesar Europe (Karlsruhe, Germany), Sigma–Aldrich (Saint Louis, MO, USA) or Merck (Darmstadt, Germany). The ternary compositions of TEOS/OTEOS/PTEOS (**TOP**), TEOS/DMDEOS/PTEOS (**TDP**) and TEOS/DMDEOS/OTEOS (**TDO**) will be used in abbreviated forms.

1.2. Synthesis of isopropyl 2-ethoxyacetate

Isopropyl 2-ethoxyacetate was prepared by the method of Oláh et al.[1]

1.3. Enzymes

CaLB for immobilization experiments (recombinant *Candida antarctica* lipase B as lyophilized powder) was obtained from c-LEcta (Leipzig, Germany), Commercial CaLB as Immobead-T2-150 (lipase B from *Candida antarctica*, covalently attached to dry acrylic) and Novozym® 435 (recombinant lipase expressed in *Aspergilus niger,* adsorbed on acrylic resin) were the purchased from Chiral Vision BV (Leiden, Netherlands) and Sigma–Aldrich (Saint Louis, MO, USA), respectively.

2. Analytical methods

2.1. NMR measurements

The NMR spectra were recorded in $CDCl_3$ on a Bruker DRX-300 spectrometer operating at 300 MHz for ^{1}H and 75 MHz for ^{13}C, and signals are given in ppm on the δ scale.

2.2. Infrared spectroscopy

Infrared spectra were recorded on a Bruker ALPHA FT-IR spectrometer and wavenumbers of bands are listed in cm^{-1}.

2.3. Optical rotation measurements

Optical rotations were measured on Perkin–Elmer 241 polarimeter at the D-line of sodium. The polarimeter was calibrated with measurements of both enantiomers of menthol.

2.4. Raman spectroscopy

A Horiba Jobin-Yvon LabRAM system coupled with external 785 nm diode laser source and Olympus BX-40 optical microscope was used for collecting Raman mapping spectra. An objective of 20× objective (laser spot size: ~3 μm) was used in focusing and spectrum acquisition. The

confocal hole of 1000 µm was employed in confocal system. In the instrument, a 950 groove/mm grating monochromator disperses the Raman photons before those reaches the CCD detector. The spectrograph position was set to provide the spectral range of 457-1678 cm^{-1} and 3 cm^{-1} resolution. Samples were put to a slide in two parts and Raman mapping was performed on the smoothed surface. The maps were collected with 50 µm step size and consisted of 21×21 points. Every single spectrum was measured with acquisition time of 60 s and 2 spectra were averaged at each measured point.

2.5. Particle size analyzer

Particle size distribution of the sol-gel entrapped CaLB preparations was determined by laser light scattering (Horiba. LA-950). The sol-gel entrapped CaLB samples were dispersed in ethanol. Ultrasonic (20 kHz) was applied to disintegrate the aggregates of the sol-gel particles. The size distribution was measured after 0. 300 and 600 s ultrasonication. Mie scattering theory was used in the calculations.[2]

2.6. Scanning electron microscopy (SEM)

The morphology of different sol-gel preparations was analyzed by a JEOL JSM-5500LV scanning electron microscope (SEM). For better imaging samples were coated with a gold nano-film layer by a neubliser.

2.7. BET apparatus (nitrogen adsorption/desorption)

Nitrogen adsorption/desorption isotherms were measured at -196 °C with a Nova2000e (Quantachrome) computer controlled apparatus. Samples were degassed at 20 °C for 24 h. The apparent surface area SBET was calculated using the Brunauer–Emmett–Teller (BET) model.[3] The total pore volume (V_{tot}) was derived from the amount of nitrogen adsorbed at relative pressure 0.95, assuming that the pores are then filled with liquid adsorbate. The micropore volume (W_0) was derived from the Dubinin–Radushkevich (DR) plot.[4] The average diameter was calculated assuming open end cylindrical pores. The density of the samples was measured by He pycnometry (Quantachrome).

2.8. Gas chromatography (GC) of CaLB catalyzed kinetic resolutions

The reaction mixtures form different kinetic resolutions (KR) were analyzed on an Agilent 4890 GC instrument equipped with flame ionization detector (FID, 250 °C) and a Hydrodex β-6TBDM column [25 m × 0.25 mm with 0.25 µm film thickness of heptakis-(2,3-di-*O*-methyl-6-*O*-*t*-butyl-dimethylsilyl)-β-cyclodextrin phase], injector temperature 250 °C, carrier gas H_2, head pressure 12 psi, split ratio 1:50 and on an Agilent 5890 GC instrument equipped with FID (250 °C) and a Hydrodex β-TBDAc column [25 m × 0.25 mm with 0.25 µm film thickness of heptakis-(2,3-di-*O*-acetyl-6-O-t-butyl-dimethylsilyl)-β-cyclodextrin phase], injector temperature 250 °C, carrier gas H_2, head pressure 12 psi, split ratio 1:50.

*2.9. Synthesis of racemic 2-ethoxy-N-(heptan-2-yl)acetamide (rac-***4b***) as GC standard*

2-Ethoxyacetyl chloride was synthesized according to the a slightly modified method of Yuan et al.[5] 2-Ethoxyacetic acid (207 mg, 1.985 mmol, 203 µL) in dry dichloromethane (10 mL) was added into pre-dried round bottom flask (50 mL) and cooled to 0 °C. A solution of thionyl chloride (1.0 equiv.; 236 mg, 1.985 mmol, 144 µL) and dichloromethane (10 mL) was added dropwise and the resulted mixture was stirred at 0 °C for 1 h and at RT for 2 h. After removal of the volatile components in vacuum (final pressure of 15 mbar at 40°C), the residue was dissolved in toluene (10 mL) and re-evaporated under vacuum (final pressure of 15 mbar at 40°C; this step was repeated twice). The formed 2-ethoxyacetyl chloride (colorless liquid, 173 mg, 1.412 mmol, 70%) was directly reacted with racemic amine *rac*-**3b** to form *rac*-**4b**.

To the mixture of racemic amine *rac*-**3b** (162 mg, 1.41 mmol), triethylamine (1.5 equiv., 214 mg, 2.118 mmol, 295 µL) and dry dichloromethane (10 mL) was added 2-ethoxyacetyl chloride (1.0 equiv.; 173 mg, 1.412 mmol) at 0 °C and the resulted mixture was stirred at 0 °C for 1 h and at RT for 16 h. After removal of the volatile components in vacuum (final pressure of 15 mbar at 40°C), the residue was dissolved in toluene (10 mL) and extracted with hydrochloric acid (2 × 5 mL, 20%). The organic phase was washed with saturated brine (10 mL), dried over Na_2SO_4 and evaporated under vacuum. The product *rac*-**4b** was isolated from the residue by preparative silica gel plate chromatography (eluent dichloromethane, R_f *rac*-**4b**= 0.67) in 16% yield as colorless liquid.

2-Ethoxy-N-(heptan-2-yl)acetamide, *rac*-**4b**

Yield: 45 mg (16%); R_f (5% CH_3OH/CH_2Cl_2) 0.80; ^{1}H-NMR, δ_H (300 MHz. $CDCl_3$): 0.97-0.79 (3H, t, J=7.0, CH_3); 1.16 (3H, d, J=6.6, CH_3); 1.28 (9H, dq, J_1=14.1. J_2=7.0, J_3=6.6 Hz, 3×CH_2. CH_3); 3.57 (2H, q. J=7.0. CH_2); 3.91 (2H, s, CH_2); 4.02 (1H, dq, J_1=8.9, J_2=6.6 Hz CH); 6.34 (1H, s, NH); ^{13}C-NMR, δ_C (75 MHz, $CDCl_3$) 169.01, 69.97, 67.06, 44.63, 36.87, 31.66, 25.67, 22.55, 20.95, 15.05, 14.00; IR, ν_{max} (film): 3414 and 3306 (NH), 2959-2858 (CH), 1654 (CO), 1522 (NH), 1449 and 1379 (CH_2), 1115 (COC) cm^{-1}.

3. Experimental methods

3.1. Scaled-up CaLB immobilization

Immobilization was performed in a 1 L beaker in a similar manner as described in the Experimental section of the main article but using all components in hundred times higher amounts.

3.2. Evaluation of the catalytic properties of the sol–gel entrapped CaLB biocatalysts

Conversion (c), enantiomeric excess (ee) and enantiomeric ratio (E) were determined by using GC data. Enantiomeric ratio (E) was calculated from c and ee_P of the product using the equation $E = \ln[1-c(1+ee_P)]/\ln[1-c(1-ee_P)]$,[6] where – as products – P stands for (*R*)-**2a**, (*R*)-**2b**, (*R*)-**4a** or (*R*)-**4b**.

To characterize the productivity of the biocatalysts. the specific reaction rates in batch reactions (r_{batch}) were calculated using the equation $r_{batch} = n_P/(t \times m_B)$ (where n_P [µmol] is the amount of the product. t [min] is the reaction time and m_B [g] is the mass of the applied biocatalyst).[7] The specific reaction rates in continuous-flow systems (r_{flow}) were calculated using the equation $r_{flow} = [P] \times v/m_B$ (where $[P]$ [mol mL^{-1}] is the molar concentration of the product, v [mL min^{-1}] is the flow rate and m_B [g] is the mass of the applied biocatalyst).[7]

3.3. Representative GC data and chromatograms for the CaLB-catalyzed KRs

Table S1. GC analysis of the products of CaLB-catalyzed kinetic resolutions

KR	Oven program	Column	Compound	t_R (min)	Ref. chrom.
rac-**1a**	120 °C isothermal, 8 min	Hydrodex β-6TBDM	(*S*)-**2a**	3.31	FigS1.
			(*R*)-**2a**	3.57	
			(*R*)-**1a**	4.46	
			(*S*)-**1a**	4.66	
rac-**1b**	50–150 °C, 10 °C min^{-1}	Hydrodex β-6TBDM	(*R*,*S*)-**1b**	6.22	FigS2.
			(*S*)-**2b**	6.51	
			(*R*)-**2b**	7.01	
rac-**3a**	100-180 °C, 8 °C min^{-1}, 5 min 180 °C	Hydrodex β-TBDAc	(*S*)-**3a**	2.82	FigS3.
			(*R*)-**3a**	2.97	
			(*R*,*S*)-**4a**	10.74	
	100-180 °C, 4 °C min^{-1}, 5 min 180 °C	Hydrodex β-6TBDM	(*S*)-**4a**	17.38	FigS4.
			(*R*)-**4a**	17.64	
rac-**3b**	5 min 100 °C, 100-142 °C, 3 °C min^{-1}. 142-182 °C. 10 °C min^{-1}	Hydrodex β-TBDAc	(*R*,*S*)-**3b**	1.32	FigS5
			(*R*,*S*)-**4b**	17.62	
	100–160 °C, 4 °C min^{-1}, 160–180 °C, 20 °C min^{-1} 1 min at 180 °C	Hydrodex β-6TBDM	(*S*)-**4b**	11.66	FigS6.
			(*R*)-**4b**	11.92	

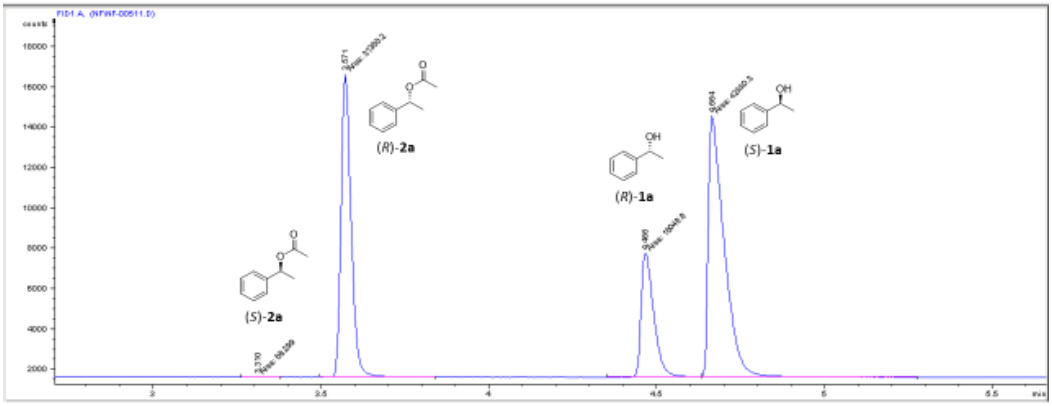

#	Time	Area	Height	Width	Area%	Symmetry
1	3.31	68.3	30.7	0.0371	0.076	0.982
2	3.571	31360.2	15058.9	0.0347	34.835	0.694
3	4.466	16046.6	6155.3	0.0434	17.825	0.52
4	4.664	42550.3	12977.4	0.0546	47.265	0.296

Fig. S1. KR of *rac*-**1a** catalyzed by **TOP**-10 CaLB, reaction time 1h.

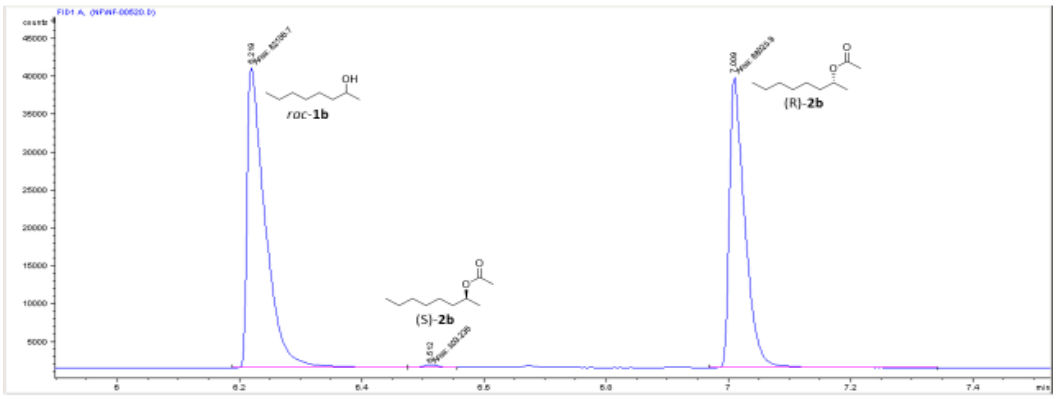

#	Time	Area	Height	Width	Area%	Symmetry
1	6.219	82106.7	39761.6	0.0344	54.507	0.313
2	6.512	503.2	313.3	0.0268	0.334	0.861
3	7.009	68025.9	38533.2	0.0294	45.159	0.444

Fig. S2. KR of *rac*-**1b** catalyzed by **TOP**-10 CaLB, reaction time 1h.

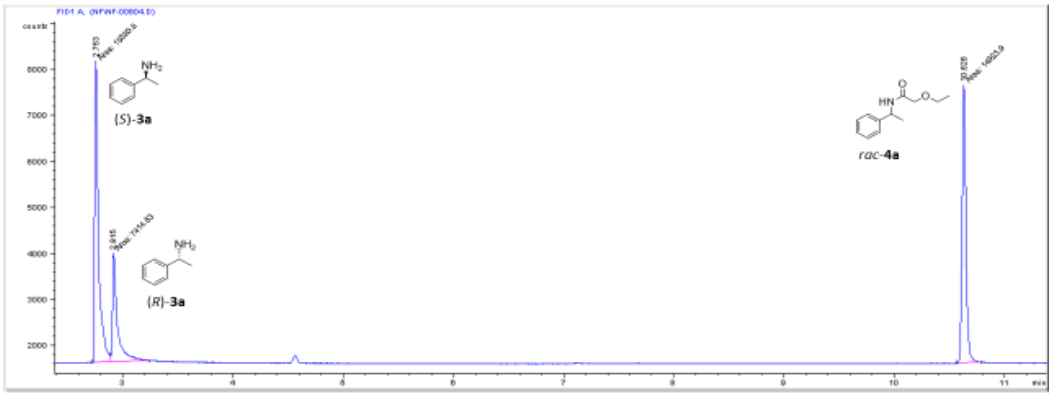

#	Time	Area	Height	Width	Area%	Symmetry
1	2.753	15350.5	6569.6	0.0389	40.729	0.401
2	2.915	7414.8	2374	0.0521	19.674	0.329
3	10.626	14923.9	6053.4	0.0411	39.597	0.776

Fig. S3. KR of *rac*-**3a** catalyzed by **TDP**-6 CaLB, reaction time 1h.

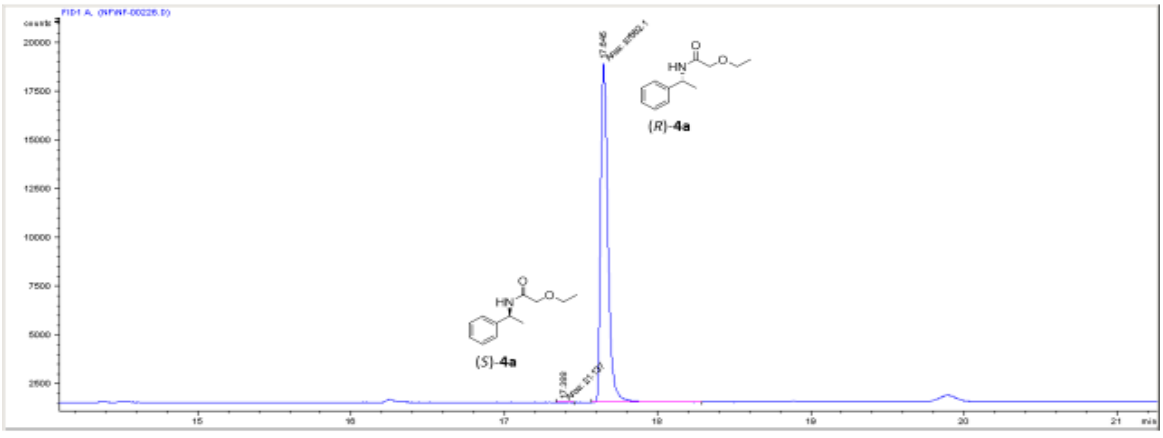

#	Time	Area	Height	Width	Area%	Symmetry
1	17.388	21.1	6.2	0.0572	0.037	0.568
2	17.645	57662.1	17438.4	0.0551	99.963	0.63

Fig. S4. KR of *rac*-**3a** catalyzed by **TDP**-6 CaLB, reaction time 1h.

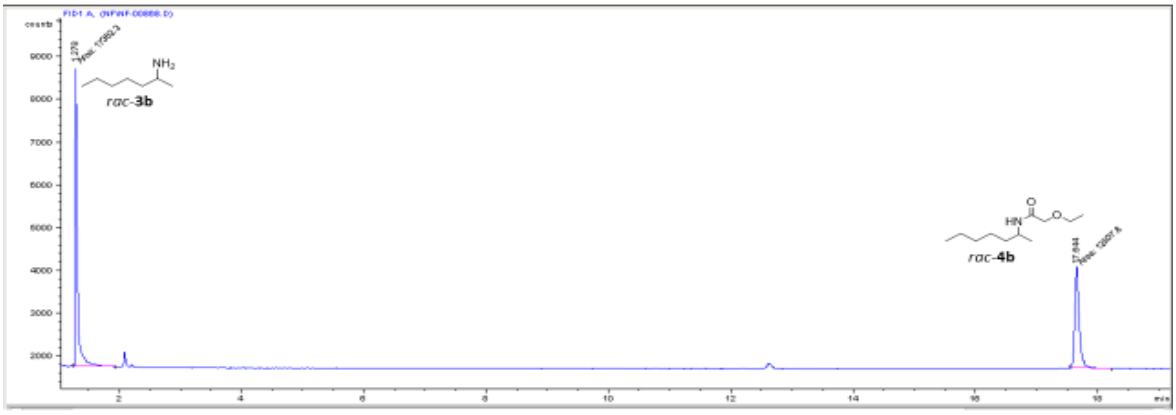

#	Time	Area	Height	Width	Area%	Symmetry
1	1.278	17362.3	7034.9	0.0411	58.126	0.307
2	17.644	12507.8	2375.3	0.0878	41.874	0.62

Fig. S5. KR of *rac*-**3b** catalyzed by **TDP**-8 CaLB, reaction time 1h.

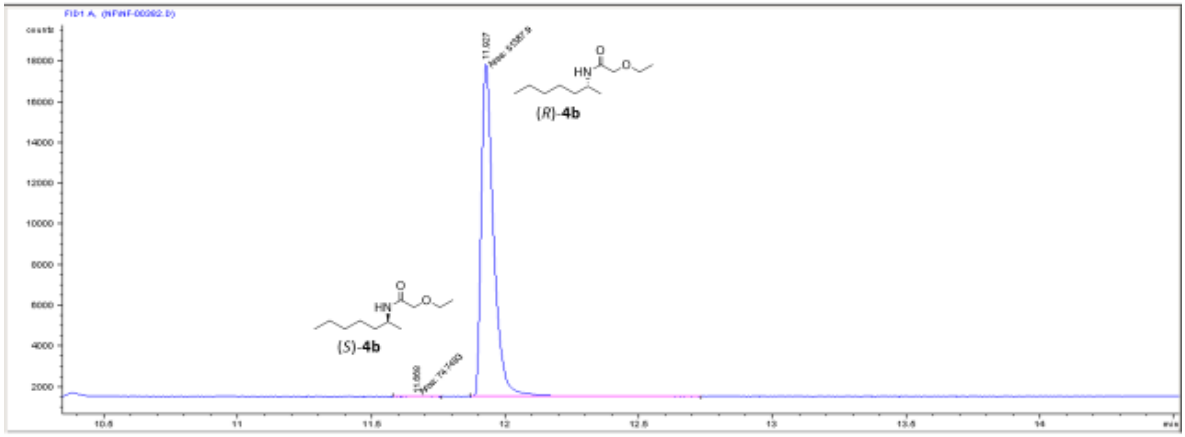

#	Time	Area	Height	Width	Area%	Symmetry
1	11.668	74.7	21.7	0.0573	0.145	0.852
2	11.927	51387.9	16389.4	0.0523	99.855	0.563

Fig. S6. KR of *rac*-**3b** catalyzed by **TDO**-8 CaLB, reaction time 1h.

3.4. Reuse of immobilized CaLB biocatalysts

CaLB biocatalyst (50 mg) was added to the solution of *rac*-**1a** (100 µL) and vinyl acetate (200 µL) in n-hexane:MTBE 2:1 (2 mL), and the resulting mixture was shaken at 30 °C in a closed 4 mL glass vial at 750 rpm for 1 h. Samples were taken after 1 h and after dilution with ethanol (975 µL) analyzed by GC. After one cycle, the *Ca*LB preparation was washed with 2-propanol (2 x 5 mL) and *n*-hexane (5 mL) and dried at RT for 2 h. The reactions with each biocatalyst were repeated in 10 cycles under identical conditions (keeping constant proportion of the components: CaLB preparation/*rac*-**1a**/vinyl acetate/*n*-hexane:MTBE 2:1 = 1/2/4/40). Samples (25 µL) were taken and after dilution with 975 µL of EtOH analyzed by GC (Section 2.6 in ESI).

3.6. Thermal stability of the biocatalysts in batch mode

The *Ca*LB biocatalysts (25 mg) in toluene (0.5 mL) were kept at the given temperatures (30, 40, 50, 60, 70, 80, 90 or 100 °C) for 1 h using Thermomixer comfort as a heat transfer medium. After 1 h, a solution of *rac*-**1a** (50 µL) and vinyl acetate (100 µL) in toluene (350 µL) was added to the reaction mixtures. Test reactions were performed at the same temperature as the thermal treatment for 0.5 h. Samples (25 µL) were taken after 0.5 h and after dilution (with 975 µL of ethanol) analyzed by GC (see Section 3.4 in ESI).

4. Molecular modeling methods

The two X-ray structures of CaLB [PDB ID: 5A6V chain A (with open-lid conformation) and chain B (with closed-lid conformation)] were completed and adjusted using the Protein Preparation Wizard,[8] as described earlier.[9] The process consisted four steps: i) hydrogen atoms were added and bond orders were assigned, ii) artifacts of the protein crystallization procedure and waters were removed, iii) hydrogen bond network, tautomeric states, and ionization states were determined and optimized, and iv) a constrained minimization was performed.

For computations, partially hydrolyzed forms [$Si(OEt)_2(OH)_2$, $RSi(OEt)(OH)_2$, and $R_2Si(OEt)(OH)$] of tetraethoxysilane, monosubstituted triethoxysilanes [$RSi(OEt)_3$, R= methyl, vinyl, *n*-propyl, *n*-hexyl, *n*-octyl, *n*-decyl, *n*-dodecyl, *n*-octadecyl, phenyl], and a disubstituted diethoxysilane, dimethyl diethoxysilane were prepared. An initial set of binding poses of the partially hydrolyzed silanes bound to CaLB with open lid conformation (refined model of 5A6V: chain A) and CaLB with closed lid conformation (refined model of 5A6V: chain B) were obtained by induced fit docking. Glide[10] was used to get the initial docking poses [standard precision with expanded sampling, max. minimization iterations: 200, max. number of poses per ligand: 10, receptor and ligand Van der Waals radii were scaled to 90% of the original values]. The crude structures were subjected to protein sidechain conformation prediction [with C_α-C_β vectoring that simulates small-scale backbone movement, force field: OPLS3, solvation model: chloroform with an external relative dielectric constant of 2.0, number of steps: 2] and a final minimization [force field: OPLS3, method: BFGS, solvation model: chloroform with an external relative dielectric constant of 2.0, RMSG: 0.01 kcal mol^{-1} $Å^{-1}$] using Prime.[11] The final, lowest energy binding states were selected for each ligand after rescoring with a modified version of MM-GBSA. The standard MM-GBSA method involves the minimization, incorporating also implicit solvation, of the ligand-receptor complex, followed by the subsequent minimization of the receptor and the ligand individually after separation. Finally, the MM-GBSA score (ΔE_b) is calculated according to Eq. S1,

$$\Delta E_b = E_{complex} - E_{receptor} - E_{ligand} \quad \text{(S1)}$$

where the three terms are the final energies of the previously mentioned minimizations, respectively. Our modifications involved i) the substitution of the ligand energy term in Eq S1 with a value obtained after mixed Monte Carlo/low-mode conformational search with MacroModel[12] [force field: OPLS3, solvation model: chloroform, number of steps: 2000, energy window: 31 kJ mol^{-1}] and a re-optimization with Prime[11] [used with the same settings as before], and ii) the substitution of the receptor energy term in Eq. S1 uniformly for all ligands with the corresponding

energy in the apoenzyme structure. These scores are approximations of the ligand binding Gibbs energies, thus are directly related to ligand binding affinity, are denoted throughout the text as "ΔE_b", and will be referred simply as binding energies. One should be warned that these figures should not be compared to experimental values, rather than compared to each other.

5. Experimental design

By selecting a design degree of 3 (silane precursors as independent variables) and augmenting the center and axial points, a 13 points model was offered by the statistical data analyzer program (Statistica 12,[13] Table S2). In order to provide an estimate of the experimental error and achieve more precise estimates of the components effect, the center point was duplicated (points 10 and 14 in Table S2, Figs. 1, 3). The model was applied for 3 different ternary systems, namely TEOS/OTEOS/PTEOS (**TOP**), TEOS/DMDEOS/PTEOS (**TDP**) and TEOS/DMDEOS/OTEOS (**TDO**). Preliminary investigations showed that presence of a minimum molar fraction of TEOS (x_{TEOS}= 0.12) is necessary in the organosilane precursor compositions for the gel formation. Accordingly, in the triangular layouts only the axe of TEOS represented a pure precursor component (x_{TEOS}= 0.00 in Fig. 3) and the molar fractions of the other organosilanes were set to 0.88 as a maximum (Table S2). Binary compositions, which provide estimates of second order effects, occur on the sides of the triangles (Fig. 3). The points in the interior, which were added to augment the design, represent ternary compositions.

Table S2. Degree of independent variables and component properties of the general ternary sol-gel matrix model generated by *Statistica 12*.

Points	Levels of factors (organosilanes)[a]			Molar proportions of orgaonsilanes		
	A	**B**	**C**	$x_{A(TEOS)}$	x_B	x_C
1	+2	-2	-2	1.000	0.000	0.000
2	-2	+2	-2	0.120	0.880	0.000
3	-2	-2	+2	0.120	0.000	0.880
4	0	+1	-2	0.413	0.586	0.000
5	0	-2	+1	0.413	0.000	0.586
6	-1	0	+1	0.120	0.293	0.586
7	+1	0	-2	0.706	0.293	0.000
8	+1	-2	0	0.706	0.000	0.293
9	-2	+1	0	0.120	0.586	0.293
10	0	0	0	0.413	0.293	0.293
11	+1	-1	-1	0.706	0.146	0.146
12	-1	+1	-1	0.266	0.586	0.146
13	-1	-1	+1	0.266	0.146	0.586
14	0	0	0	0.413	0.293	0.293

[a] 3 Factor simplex-lattice design (Degree m=3) + interior points and overall centroid. $x_{B.C}$: can be OTEOS. PTEOS or DMDEOS.

5.1. Significant parameters for biocatalytic activities

Table S3. Significant variables and significant interactions (marked with green) on the r_{batch} as dependent variables in the KR of *rac*-**1a** catalyzed by *Ca*lB entrapped in **TOP** (Panel A), **TDP** (Panel B) and **TDO** (Panel C) sol-gel systems.

Factor	Coefficient	Standard error	t	p	Confidence limit	
					-95 %	+95 %
Panel A[a]						
(A)TEOS	-4.5760	10.41355	-0.439428	0.671980	-28.590	19.4377
(B)OTEOS	4.4607	10.41355	0.428360	0.679689	-19.553	28.4744
(C)PTEOS	38.7776	10.41355	3.723760	0.005840	14.764	62.7913
AB	106.3301	45.09260	2.358039	0.046099	2.346	210.3138
AC	65.7552	45.09260	1.458227	0.182890	-38.228	169.7390
BC	-12.5117	45.09260	-0.277466	0.788457	-116.495	91.4720
Panel B[b]						
(A)TEOS	-9.15280	10.81231	-0.846516	0.415301	-32.9505	14.64493
(B)DMDEOS	68.26460	10.81231	6.313601	0.000057	44.4669	92.06233
(C)PTEOS	39.71677	10.81231	3.673293	0.003668	15.9190	63.51450
Panel C[c]						
(A)TEOS	6.610	8.49830	0.77775	0.459097	-12.988	26.2067
(B)DMDEOS	76.049	8.49830	8.94875	0.000019	56.452	95.6463
(C)OTEOS	9.293	8.49830	1.09357	0.305975	-10.304	28.8906
AB	-100.763	36.79922	-2.73819	0.025521	-185.622	-15.9040
AC	39.947	36.79922	1.08553	0.309311	-44.912	124.8058
BC	-7.268	36.79922	-0.19749	0.848366	-92.127	77.5915

[a]MS Residual= 130.0158. [b]MS Residual= 278.8425. [c]MS Residual= 86.5890

Table S4. Significant variables and significant interactions (marked with green) on the r_{batch} as dependent variables in the KR of *rac*-**1b** catalyzed by CaLB entrapped in: **TOP** (Panel A), **TDP** (Panel B) and **TDO** (Panel C) sol-gel systems.

Factor	Coefficient	Standard error	t	p	Confidence limit	
					-95 %	+95 %
Panel A[a]						
(A)TEOS	-1.728	6.0317	-0.28651	0.782785	-15.991	12.5346
(B)OTEOS	2.257	6.0317	0.37419	0.719343	-12.006	16.5197
(C)PTEOS	71.228	6.0317	11.80896	0.000007	56.966	85.4911
AB	82.520	28.8847	2.85686	0.024447	14.218	150.8209
AC	-50.346	28.8847	-1.74301	0.124860	-118.648	17.9552
BC	-138.470	28.8847	-4.79388	0.001980	-206.771	-70.1682
ABC	434.864	166.0631	2.61866	0.034476	42.187	827.5405
Panel B[b]						
(A)TEOS	0.278	7.70862	0.03604	0.972137	-17.498	18.0539
(B)DMDEOS	70.259	7.70862	9.11440	0.000017	52.483	88.0355
(C)PTEOS	2.617	7.70862	0.33950	0.742976	-15.159	20.3931
AB	-104.507	33.37973	-3.13085	0.013997	-181.481	-27.5331
AC	70.685	33.37973	2.11760	0.067075	-6.289	147.6588
BC	-3.582	33.37973	-0.10730	0.917196	-80.555	73.3923
Panel C[c]						
(A)TEOS	2.874	15.68193	0.18328	0.859135	-33.288	39.0369
(B)DMDEOS	72.850	15.68193	4.64547	0.001654	36.687	109.0125
(C)OTEOS	65.981	15.68193	4.20744	0.002966	29.818	102.1434
AB	-79.984	67.90566	-1.17787	0.272698	-236.575	76.6068
AC	-52.956	67.90566	-0.77985	0.457929	-209.547	103.6346
BC	-175.558	67.90566	-2.58532	0.032347	-332.149	18.9673

[a]MS Residual= 42.3166. [b]MS Residual= 71.24447. [c]MS Residual= 294.8475

Table S5. Significant variables and significant interactions (marked with green) on the r_{batch} as dependent variables in the KR of *rac*-**3a** catalyzed by CaLB entrapped in **TOP** (Panel A), **TDP** (Panel B) and **TDO** (Panel C) sol-gel systems.

Factor	Coefficient	Standard error	t	p	Confidence limit	
					-95 %	+95 %
Panel A[a]						
(A)TEOS	88.20746	37.48184	2.353339	0.038261	5.7105	170.7044
(B)OTEOS	93.737321	37.481841	2.5008731	0.029461	11.2403	176.2343
(C)PTEOS	22.85791	37.48184	0.609840	0.554357	-59.6391	105.3549
Panel B[b]						
(A)TEOS	17.0437	39.3431	0.433206	0.676308	-73.682	107.7691
(B)DMDEOS	124.0129	39.3431	3.152084	0.013556	33.287	214.7383
(C)PTEOS	-10.2016	39.3431	-0.259298	0.801953	-100.927	80.5238
AB	-83.4399	170.3630	-0.489777	0.637439	476.298	309.4179
AC	404.4471	170.3630	2.374031	0.044963	11.589	797.3049
BC	440.3052	170.3630	2.584512	0.032388	47.447	833.1630
Panel C[c]						
(A)TEOS	30.8259	38.34187	0.803975	0.438441	-53.5640	115.2158
(B)DMDEOS	87.74171	38.34187	2.288403	0.042898	3.3518	172.1316
(C)OTEOS	143.0702	38.34187	3.731435	0.003315	58.6803	227.4601

[a]MS Residual= 3350.919. [b]MS Residual= 1855.821. [c]MS Residual= 3506.459

Table S6. Significant variables and significant interactions (marked with green) on the r_{batch} as dependent variables in the KR of *rac*-**3b** catalyzed by CaLB entrapped in: **TOP** (Panel A), **TDP** (Panel B) and **TDO** (Panel C) sol-gel systems.

Factor	Coefficient	Standard error	t(8)	p	Confidence limit	
					-95 %	+95 %
Panel A[a]						
(A)TEOS	73.77890	41.33214	1.785025	0.101826	-17.1925	164.7503
(B)OTEOS	74.737211	41.332141	1.8082101	0.0979641	-16.2342	165.7086
(C)PTEOS	38.24278	41.33214	0.925255	0.374686	-52.7287	129.2142
Panel B[b]						
(A)TEOS	14.23	24.3586	0.58400	0.590565	-53.40	81.856
(B)DMDEOS	79.13	24.3586	3.24864	0.031416	11.50	146.762
(C)PTEOS	6.48	24.3586	0.26607	0.803335	-61.15	74.111
AB	-161.02	108.9174	-1.47838	0.213384	-463.42	141.382
AC	338.62	108.9174	3.10892	0.035909	36.21	641.019
BC	394.53	108.9174	3.62233	0.022311	92.13	696.938
ABC	-1249.87	623.3635	-2.00505	0.115450	-2980.61	480.862
AB(A-B)	78.32	208.6620	0.37532	0.726474	-501.02	657.654
AC(A-C)	606.84	208.6620	2.90822	0.043756	27.50	1186.174
BC(B-C)	-493.61	208.6620	2.36560	0.077190	-1072.95	85.727
Panel C[c]						
(A)TEOS	24.48149	25.96370	0.942912	0.365975	-32.6642	81.6272
(B)DMDEOS	52.56087	25.96370	2.024398	0.067901	-4.58491	109.7066
(C)OTEOS	89.73206	25.96370	3.456058	0.005370	32.5863	146.8778

[a]MS Residual= 4074.722, [b]MS Residual= 596.2758, [c]MS Residual= 1607.887

5.2. The residuals and distribution function of biocatalytic activities

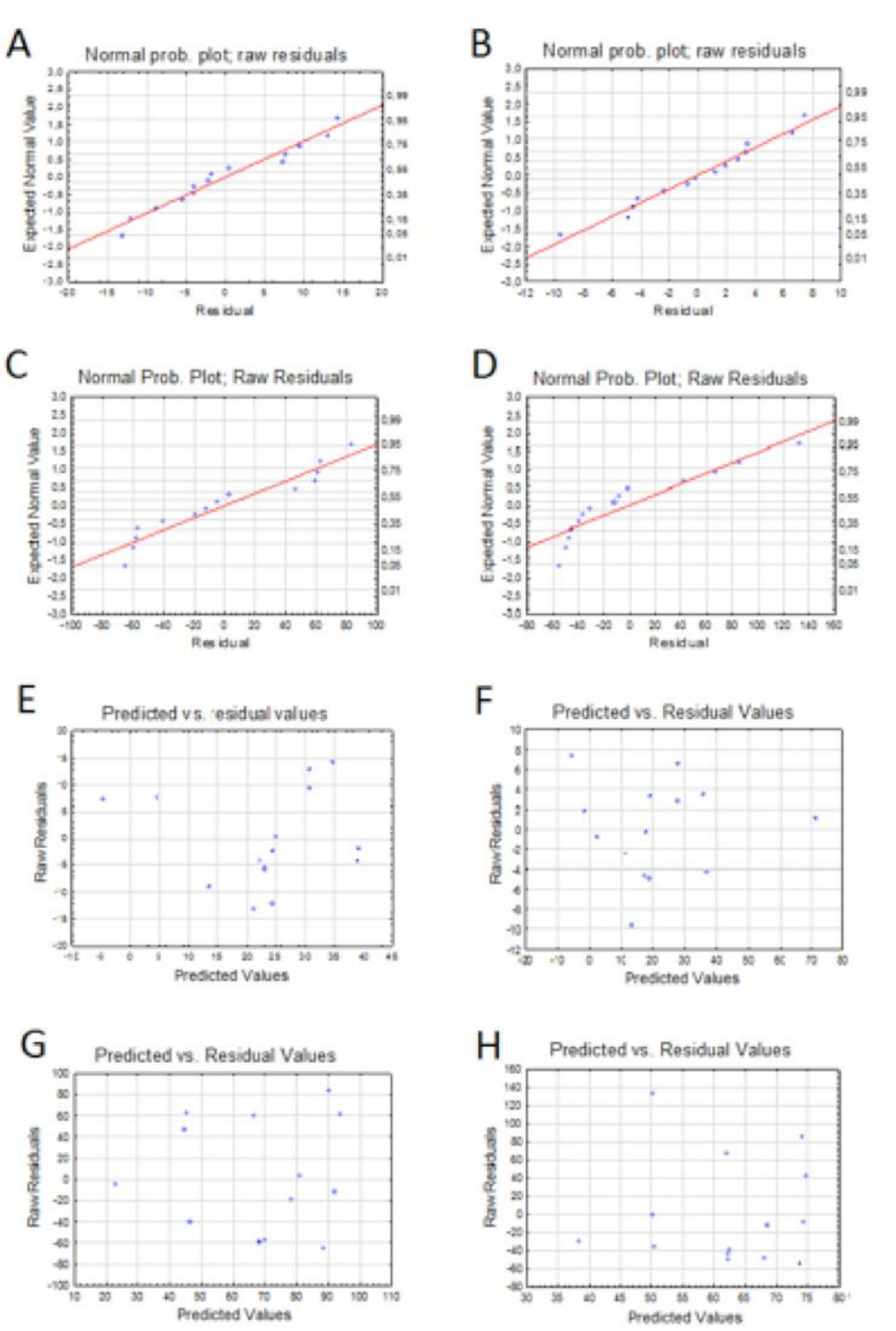

Fig. S7. The residuals of r_{batch} *rac*-**1a** (A), *rac*-**1b** (B), *rac*-**3a** (C) and *rac*-**3b** (D) and distribution function of r_{batch} *rac*-**1a** (E) *rac*-**1b** (F), *rac*-**3a** (G) and *rac*-**3b** (H) in **TOP** CaLB system.

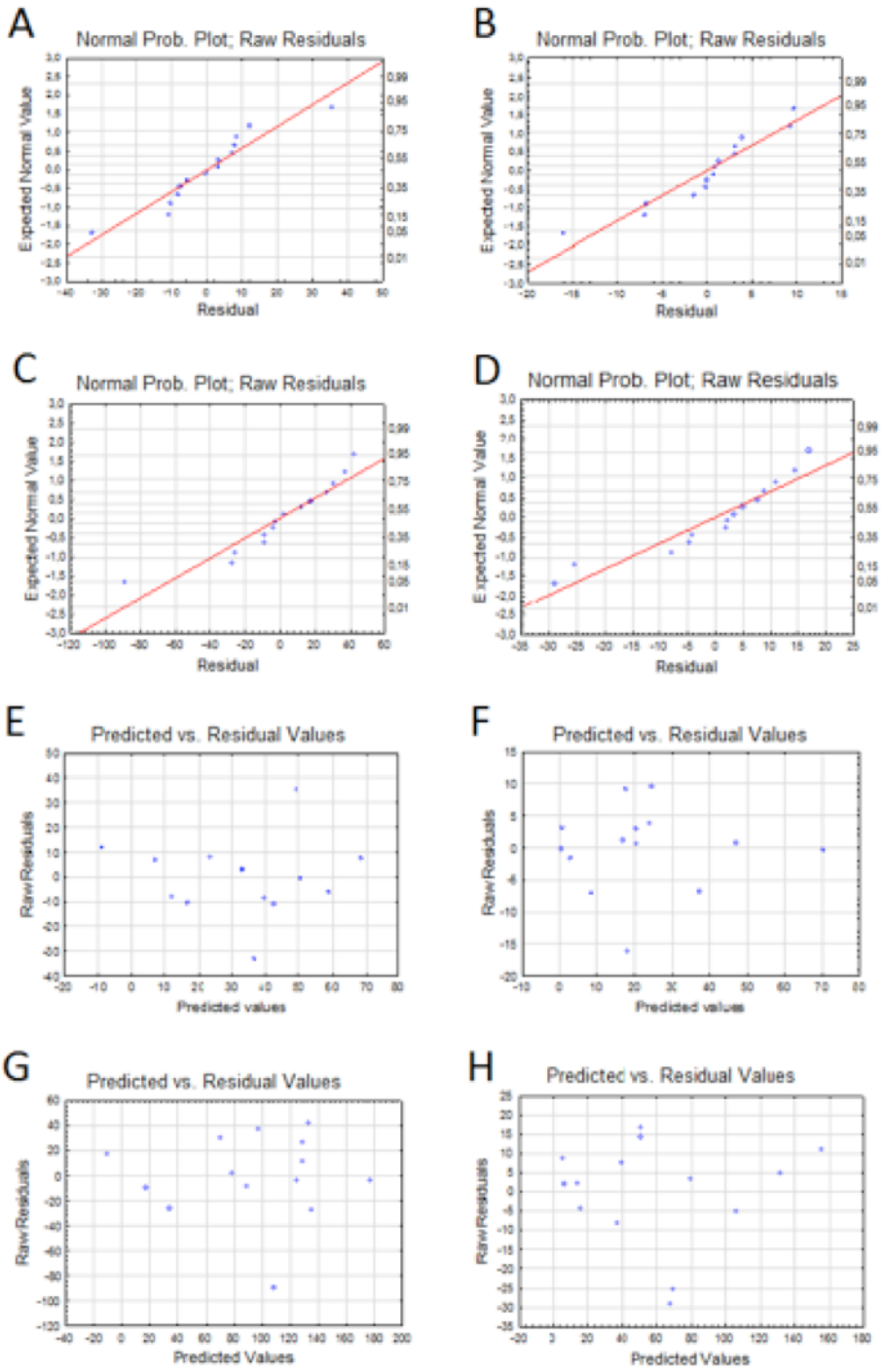

Fig. S8. The residuals of r_{batch} *rac*-**1a** (A), *rac*-**1b** (B), *rac*-**3a** (C) and *rac*-**3b** (D) and distribution function of r_{batch} *rac*-**1a** (E), *rac*-**1b** (F), *rac*-**3a** (G) and *rac*-**3b** (H) in **TDP** CaLB system.

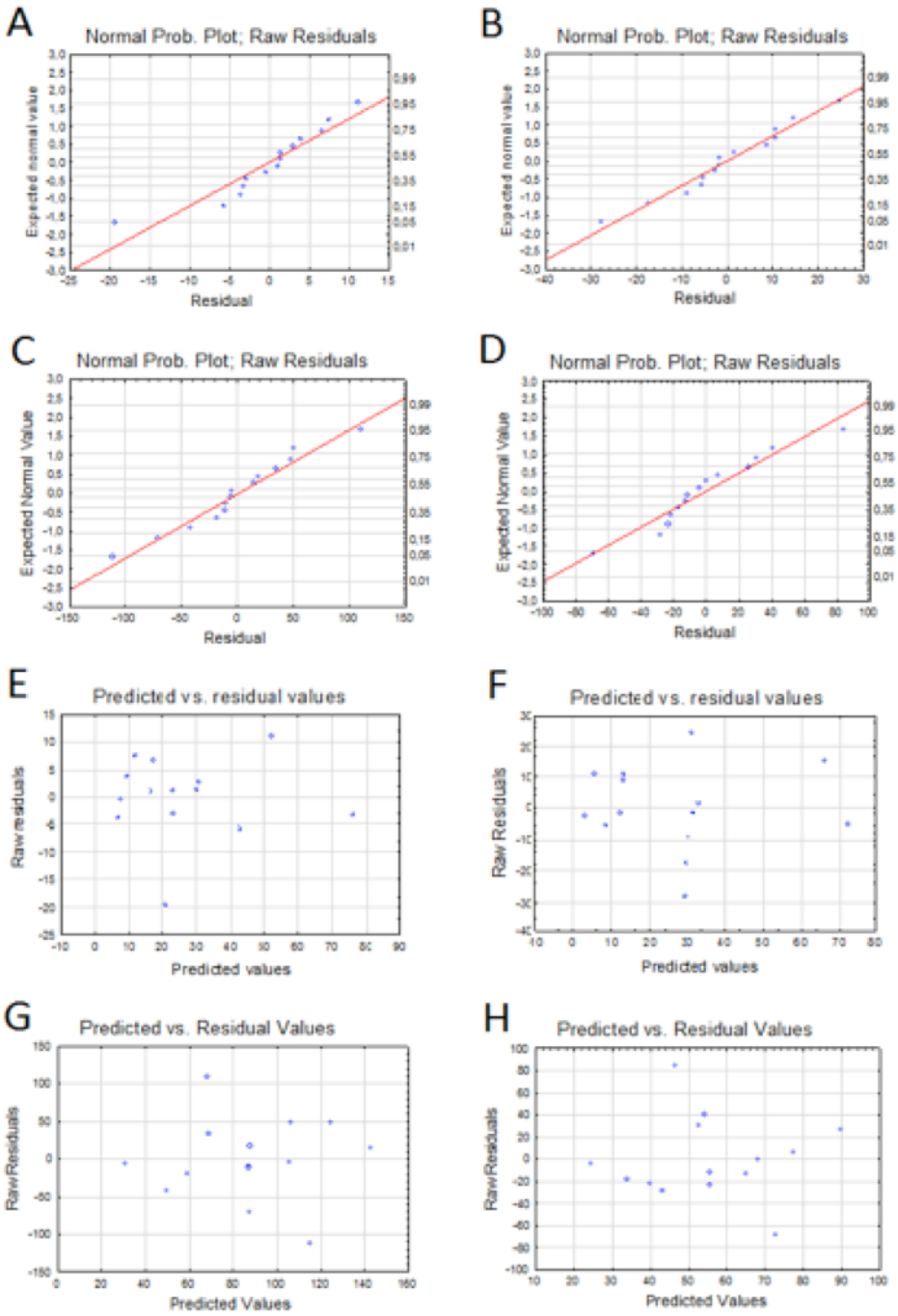

Fig. S9. The residuals of r_{batch} *rac*-**1a** (A), *rac*-**1b** (B), *rac*-**3a** (C) and *rac*-**3b** (D) and distribution function of r_{batch} *rac*-**1a** (E), *rac*-**1b** (F), *rac*-**3a** (G) and *rac*-**3b** (H) in **TDO** CaLB system.

5.3. Biocatalytic properties of sol-gel entrapped CaLB performed by experimental design

Table S7. Conversion (*c*), enantiomeric excess (*ee*) and biocatalytic activity (r_{batch}) data in KR of racemic alcohols (*rac*-**1a,b**) and amines (*rac*-**3a,b**) with CaLB biocatalysts prepared as experimental design points of **TOP** sol-gel system (reaction time 1 h).

Point	x_{TEOS}	x_{OTEOS}	x_{PTEOS}	c_{1a} (%)	$ee_{(S)\text{-}2a}$ (%)	r_{batch} (U g^{-1})	c_{1b} (%)	$ee_{(S)\text{-}2b}$ (%)	r_{batch} (U g^{-1})	c_{3a} (%)	$ee_{(S)\text{-}4a}$ (%)	r_{batch} (U g^{-1})	c_{3b} (%)	$ee_{(S)\text{-}4b}$ (%)	r_{batch} (U g^{-1})
1	1.000	0.000	0.000	1.0	[a]	2.7	0.1	[a]	0.2	4.1	99.9	22.8	3.3	99.7	18.8
2	0.120	0.880	0.000	4.3	99.0	12.0	34.5	99.7	72.4	28.2	99.9	155.2	20.1	99.7	116.3
3	0.120	0.000	0.880	12.6	99.4	34.6	0.7	[a]	1.5	3.3	99.8	17.9	1.3	[a]	7.7
4	0.413	0.586	0.000	9.2	99.1	25.5	18.7	99.8	39.2	14.5	99.9	80.0	11.4	99.8	65.8
5	0.413	0.000	0.586	13.5	99.5	37.1	10.8	98.9	22.6	16.6	99.9	91.2	8.4	99.7	48.8
6	0.120	0.293	0.586	8.1	99.4	22.3	0.9	[a]	1.9	1.1	[a]	6.3	2.4	99.5	13.8
7	0.706	0.293	0.000	6.5	99.3	18.0	4.3	99.6	9.0	31.5	99.9	173.2	27.5	99.8	159.3
8	0.706	0.000	0.293	4.5	99.5	12.4	8.4	99.4	17.7	22.9	99.9	125.9	22.3	99.9	129.0
9	0.120	0.586	0.293	1.5	[a]	4.3	6.2	99.3	12.9	2.4	99.8	13.3	3.9	99.8	22.8
10	0.413	0.293	0.293	15.8	99.5	43.6	14.8	99.8	31.0	1.8	[a]	10.1	2.2	99.8	12.5
11	0.706	0.146	0.146	6.3	99.2	17.4	6.7	99.7	14.0	10.7	99.9	58.7	3.5	99.8	20.2
12	0.266	0.586	0.146	2.8	98.8	7.8	15.6	99.8	32.7	15.3	99.9	84.0	9.7	99.8	56.3
13	0.266	0.146	0.586	17.8	99.5	49.0	1.8	[a]	3.9	19.6	99.9	108.1	31.5	99.3	182.5
14	0.413	0.293	0.293	14.5	99.5	40.0	16.6	99.8	34.8	1.7	[a]	9.1	3.1	99.8	17.7

[a] No enantiomeric excess data were calculated for reactions with $c < 2\%$.

Table S8. Conversion (*c*), enantiomeric excess (*ee*) and biocatalytic activity (r_{batch}) data in KR of racemic alcohols (*rac*-**1a,b**) and amines (*rac*-**3a,b**) with CaLB biocatalysts prepared as experimental design points of **TDP** ternary sol-gel system (reaction time 1 h).

Point	x_{TEOS}	x_{OTEOS}	x_{PTEOS}	c_{1a} (%)	$ee_{(S)\text{-}2a}$ (%)	r_{batch} (U g^{-1})	c_{1b} (%)	$ee_{(S)\text{-}2b}$ (%)	r_{batch} (U g^{-1})	c_{3a} (%)	$ee_{(S)\text{-}4a}$ (%)	r_{batch} (U g^{-1})	c_{3b} (%)	$ee_{(S)\text{-}4b}$ (%)	r_{batch} (U g^{-1})
1	1.000	0.000	0.000	1.0	[a]	2.8	0.1	[a]	0.2	1.4	[a]	7.9	2.9	99.7	16.5
2	0.120	0.880	0.000	27.6	99.5	76.0	33.3	99.6	70.0	21.9	99.9	120.4	14.3	99.8	82.5
3	0.120	0.000	0.880	11.4	99.7	31.3	0.5	[a]	1.1	1.3	[a]	7.3	1.5	[a]	8.6
4	0.413	0.586	0.000	11.5	99.5	31.6	13.2	99.3	27.6	18.3	99.9	100.4	2.0	[a]	11.8
5	0.413	0.000	0.586	11.5	99.4	31.6	12.8	99.2	26.8	14.5	99.8	79.9	8.1	99.6	47.0
6	0.120	0.293	0.586	30.8	99.5	84.8	16.2	99.6	34.0	31.8	99.9	174.9	28.7	99.8	165.9
7	0.706	0.293	0.000	2.2	97.9	6.2	1.7	[a]	3.5	1.5	[a]	8.2	2.5	99.9	14.7
8	0.706	0.000	0.293	5.1	99.3	14.1	8.6	99.4	18.0	24.5	99.9	134.7	23.6	99.9	136.8
9	0.120	0.586	0.293	19.2	99.3	53.0	22.7	99.9	47.7	31.5	99.9	173.5	17.5	99.6	101.2
10	0.413	0.293	0.293	13.0	99.4	35.9	11.1	96.6	23.3	28.2	99.9	154.9	11.7	99.9	67.4
11	0.706	0.146	0.146	1.4	[a]	4.0	0.7	[a]	1.5	14.6	99.9	80.3	7.6	99.9	44.0
12	0.266	0.586	0.146	18.2	99.4	50.1	14.5	97.4	30.5	19.5	99.9	107.5	4.9	99.7	28.6
13	0.266	0.146	0.586	1.3	[a]	3.6	1.0	[a]	2.0	3.4	99.8	18.9	6.6	99.6	38.4
14	0.413	0.293	0.293	13.1	99.5	36.2	10.0	96.7	20.9	25.4	99.9	139.7	11.2	99.8	64.9

[a] No enantiomeric excess data were calculated for reactions with $c < 2\%$.

Table S9. Conversion (*c*), enantiomeric excess (*ee*) and biocatalytic activity (r_{batch}) data in KR of racemic alcohols (*rac*-**1a,b**) and amines (*rac*-**3a,b**) with CaLB biocatalysts prepared as experimental design points of **TDO** ternary sol-gel system (reaction time 1 h).

Point	x_{TEOS}	x_{OTEOS}	x_{PTEOS}	c_{1a} (%)	$ee_{(S)\text{-}2a}$ (%)	r_{batch} (U g^{-1})	c_{1b} (%)	$ee_{(S)\text{-}2b}$ (%)	r_{batch} (U g^{-1})	c_{3a} (%)	$ee_{(S)\text{-}4a}$ (%)	r_{batch} (U g^{-1})	c_{3b} (%)	$ee_{(S)\text{-}4b}$ (%)	r_{batch} (U g^{-1})
1	1.000	0.000	0.000	1.1	[a]	2.9	0.1	[a]	0.2	4.6	99.9	25.3	3.5	99.7	20.1
2	0.120	0.880	0.000	26.4	99.7	72.8	32.1	99.8	67.5	19.2	99.9	105.9	14.4	99.8	83.3
3	0.120	0.000	0.880	4.8	99.0	13.2	38.4	99.7	80.6	28.7	99.9	157.6	20.1	99.8	116.1
4	0.413	0.586	0.000	12.1	99.6	33.4	14.3	99.8	30.1	18.8	99.9	103.2	2.6	99.7	15.0
5	0.413	0.000	0.586	8.6	99.2	23.8	16.5	99.6	34.7	18.3	99.9	100.7	11.7	99.8	67.6
6	0.120	0.293	0.586	11.3	99.6	31.3	5.7	99.8	11.9	31.4	99.9	172.7	14.5	99.7	84.0
7	0.706	0.293	0.000	2.5	98.1	6.9	1.3	[a]	2.8	1.5	[a]	8.2	2.8	99.7	16.5
8	0.706	0.000	0.293	6.3	99.1	17.4	4.9	99.8	10.4	32.5	99.9	178.7	22.6	99.8	130.8
9	0.120	0.586	0.293	23.0	99.8	63.3	26.7	99.8	56.1	28.3	99.9	155.8	9.0	99.8	51.8
10	0.413	0.293	0.293	8.8	99.5	24.4	11.3	99.7	23.8	13.8	99.9	75.9	5.6	99.6	32.3
11	0.706	0.146	0.146	6.9	99.2	19.1	7.7	99.9	16.2	7.3	99.9	40.3	3.1	99.9	18.1
12	0.266	0.586	0.146	13.3	99.6	36.7	10.1	99.8	21.2	3.0	99.9	16.6	16.4	99.8	94.7
13	0.266	0.146	0.586	0.5	[a]	1.4	0.6	[a]	1.2	0.6	[a]	3.5	0.7	[a]	3.8
14	0.413	0.293	0.293	7.3	99.4	20.1	10.4	99.3	21.8	14.0	99.9	76.8	7.6	99.8	44.1

[a] No enantiomeric excess data were calculated for reactions with $c < 2\%$.

6. SDS-PAGE analysis of CaLB immobilization

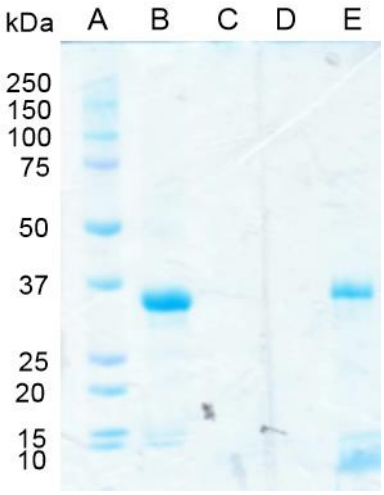

Fig. S10. SDS-PAGE analysis of CaLB preparations, colored by Coomassie Blue staining. A: protein marker. B: lyophilized CaLB in phosphate buffer (0.1 M, pH=7.5). C: washing solution after the first wash with IPA. D: washing solution after the second wash with water. E: **TDP**-10 CaLB (in amounts with enzyme content being proportional to the lyophilized CaLB.

7. Kinetic resolutions catalyzed by immobilized CaLB in continuous-flow reactor

Immobilized *Ca*LB biocatalysts were packed into stainless steel CatCart^{TM} columns (stainless steel, inner diameter: 4 mm; total length: 70 mm; packed length: 65 mm; inner volume: 0.816 mL) according to the filling process of ThalesNano Inc. The columns were settled by silver metal [Sterlitech Silver Membrane from Sigma-Aldrich, Z623237, pore size 0.45 µm; pure metallic silver, 99.97% with no extractable or detectable contaminants] and PTFE [Whatman® Sigma-Aldrich, WHA10411311, pore size 0.45 µm] filter membranes. The sealing units were made of PTFE. Filling weights of sol-gel entrapped forms of CaLB are given in the following sections for each experiments. Filling weights of commercial CaLB biocatalysts were as follows: 222.1 mg (Immobead-T2-150) and 190.0 mg (Novozym 435).

7.1. Substrate concentration dependence in the kinetic resolution of rac-1a catalyzed by sol-gel immobilized CaLB in continuous-flow reactor

The solution of *rac*-**1a** at different concentrations (1, 2.5, 5, 10, 25, 48, 64 mg mL^{-1} i.e. 0.008, 0.025, 0.041, 0.083, 0.207, 0.398, 0.531 M) and 2.76 equiv. of vinyl acetate in dry toluene was pumped through the column filled with immobilized CaLB thermostated to 30 °C at a flow rate of 0.20 mL min^{-1}. At each different reaction composition, samples were analyzed by GC every 10 min up to 40 min after the start of the experiment (the stationary operation has been established after 40 min) samples were collected and analyzed (as described in Section 3.4 in ESI). After a series of experiments, columns were washed with toluene (0.5 mL min^{-1}, 30 min) and stored in refrigerator (4 °C).

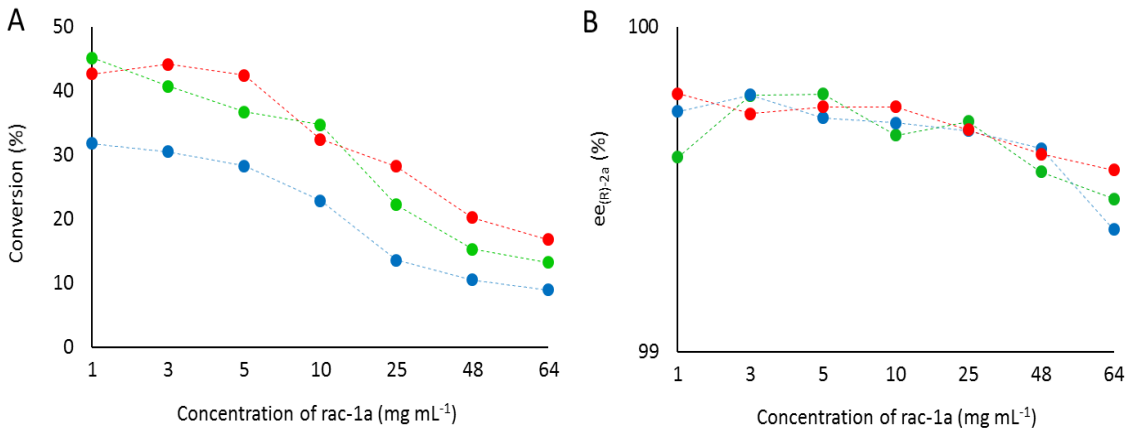

Fig. S11. Conversion (A) and enantiomeric excess of formed (*R*)-**2a** ($ee_{(R)\text{-}\mathbf{2a}}$) (B) in kinetic resolution of *rac*-**1a** at different concentrations catalyzed by ternary sol-gels: **TOP**-10 CaLB (●), **TDP**-10 CaLB (●), **TDO**-10 CaLB (●).

7.2. Continuous-flow kinetic resolution of rac-1a at different temperatures

The solution of *rac*-**1a** (0.398 M. i.e. 48 mg mL^{-1}) and vinyl acetate (2.76 equiv.) in dry toluene was pumped through the column filled with immobilized CaLB thermostated to various temperatures (30–100 °C in 10 °C steps) at a flow rate of 0.20 mL min^{-1}. The columns filled with sol-gel-entrapped CaLB were the same as in Section 7.1. At each temperature samples were analyzed by GC at every 10 min up to 40 min after the start of the experiment. After the stationary operation has been established (40 min after the start of the experiment) samples were collected (25 µL sample was diluted with ethanol to 975 µL) and analyzed as described in Section 3.4 in ESI). After a series of experiments, columns were washed with toluene (0.5 mL min^{-1}, 30 min) and stored in refrigerator (4 °C).

7.3. Production of (R)-2a, (R)-2b, (R)-4a, (R)-4b at different flow rates

The solution of the substrate (*rac*-**1a** or *rac*-**1b**, *rac*-**3a** or *rac*-**3b**, 48 mg mL^{-1}) and acylating agent (2.76 equiv. of vinyl acetate for *rac*-**1a** or *rac*-**1b** or 0.6 equiv. of isopropyl 2-ethoyxacetate for *rac*-**3a** or *rac*-**3b**) in dry toluene was pumped through the biocatalyst-filled columns (**TDP**-10 CaLB for *rac*-**1a** or *rac*-**1b**; **TDP**-11 CaLB for *rac*-**3a** or *rac*-**3b**) thermostated at 60 °C at different flow rates (0.4; 0.2; 0.1 mL min^{-1}). At each temperature, samples were analyzed by GC after the stationary operation has been established (40 min after the start of the experiment), samples were collected (25 µL sample was diluted with ethanol to 975 µL) and analyzed (as described in Section 3.4 in ESI). After a series of experiments, columns were washed with toluene (0.5 mL min^{-1}, 30 min) and stored in refrigerator (4 °C).

(*R*)-*1-Phenylethyl acetate* (*R*)-**2a**

The solution of racemic 1-phenylethanol (*rac*-**1a**, 48 mg mL^{-1}) and vinyl acetate (2.76 equiv.) in toluene was pumped through the enzyme-filled column (**TOP**-10 CaLB, filling weight: 250.2 mg) thermostated to 60 °C at a flow rate of 0.10 mL min^{-1}. After stationary operation has been

established (40 min after the start of experiment), sample was collected for 120 min. Solvents and other volatiles were removed under vacuum of 5.6 mL collected sample and compounds were separated by silica plate chromatography (eluent hexane:ethyl acetate = 10:4, R_f= 0.90). Title compound (*R*)-**2a** was obtained as light yellow liquid (Yield: 171 mg, 47%, Table S10, Entry 1).

(*R)-Octan-2-yl acetate* (*R*)-**2b**

The solution of racemic octan-2-ol (*rac*-**2a**, 48 mg mL^{-1}) and vinyl acetate (2.76 equiv.) in toluene was pumped through the enzyme-filled column (**TDP**-10 CaLB, filling weight: 225.0 mg) thermostated to 60 °C at a flow rate of 0.20 mL min^{-1}. After stationary operation has been established (40 min after the start of experiment), sample was collected for 120 min. Solvents and other volatiles were removed under vacuum of 7.9 mL collected sample and compounds were separated by silica plate chromatography (eluent hexane:ethyl acetate = 10:4, R_f= 0.85). Title compound (*R*)-**2b** was obtained as light yellow liquid (Yield: 240 mg, 48%, Table S10, Entry 2).

(*R)-2-Ethoxy-N-(1-phenylethyl)acetamide* (*R*)-**4a**

The solution of racemic 1-phenylethyanamine (*rac*-**3a**, 48 mg mL^{-1}) and isopropyl 2-ethoxyacetate (0.60 equiv.) in toluene was pumped through the enzyme-filled column (**TOP**-11 CaLB, filling weight: 241.9 mg) thermostated to 60 °C at a flow rate of 0.10 mL min^{-1}. After stationary operation has been established (40 min after the start of experiment), sample was collected for 120 min. Solvents and other volatiles were removed under vacuum of 6.0 mL collected sample, the residue was picked up in toluene (20 mL) and hydrochloric acid (20%, 20 mL) was added to this solution and after the mixture was stirred for 20 min at RT. The phases were separated and the aqueous phase was extracted with toluene (2×10 mL). The combined organic phase was washed with saturated brine (20 mL), dried over $MgSO_4$ and volatiles were removed under vacuum. Title compound (*R*)-**4a** was obtained as off white powder after crystallization from Et_2O (Yield: 223 mg. 47%, Table S10, Entry 3).

(*R*)-*2-Ethoxy-N-(heptan-2-yl)acetamide* (*R*)-**4b**

The solution of heptan-2-amine *rac*-**3b** (48 mg mL^{-1}) and isopropyl 2-ethoxyacetate (0.60 equiv.) in toluene was pumped through the enzyme-filled column (**TDO**-11 CaLB, filling weight: 225.0 mg) thermostated to 60 °C at a flow rate of 0.10 mL min^{-1}. After stationary operation has been established (40 min after the start of experiment), sample was collected for 120 min. Solvents and other volatiles were removed under vacuum from 6.0 mL collected sample, the residue was picked up in toluene (20 mL) and hydrochloric acid (20%. 20 mL) was added to this solution and after the mixture was stirred for 20 min at RT. The phases were separated and the aqueous phase was extracted with toluene (2×10 mL). The combined organic phase was washed with saturated brine (20 mL), dried over $MgSO_4$ and volatiles were removed under vacuum. Title compound (*R*)-**4b** were obtained as off white powder after crystallization from Et_2O (Table S10, Entry 4).

Yield: 235 mg, 47%; R_f (5% CH_3OH/CH_2Cl_2) 0.80; $[\alpha]_D^{20}$ +3.5 (*c* 1, CH_2Cl_2); $ee_{(R)\text{-}\mathbf{4b}}$= 99.0% (GC on Hydrodex β-TBDM column); d_H (300 MHz. $CDCl_3$): 0.89 (3H, t, *J*=6.4, CH_3); 1.16 (3H, d, *J*=6.6, CH_3); 1.21–1.36 (9H, m, 3×CH_2, CH_3); 1.43 (2H, d, *J*=6.7, CH_2); 3.91 (2H, s, CH_2); 4.02 (1H, dq, J_1=15.3, J_2=6.7, CH); 6.33 (1H, s, NH); d_C (75 MHz, $CDCl_3$) 169.01, 69.97, 67.06, 44.63, 36.87, 31.66, 25.67, 22.55, 20.95, 15.05, 14.00; IR absorptions (liquid film): v_{max} 3414 and 3306 (NH), 2959-2858 (CH), 1654 (CO), 1522 (NH). 1449 and 1379 (CH_2), 1115 (COC) cm^{-1}.

Table S10. Continuous-flow kinetic resolution of *rac*-**1a**, *rac*-**1b**, *rac*-**3a** and *rac*-**3b** (48 mg mL^{-1}) catalyzed by sol-gel immobilized *Ca*LB preparations at 60 °C in toluene.

No.	Substrate	Biocatalyst	Flow rate [mL min^{-1}]	Sample			Isolated product	
				Conversion[a] [%]	r_{flow}[a] [µmol min^{-1} g^{-1}]	$ee_{(R)\text{-product}}$[a] [%]	Yield [%]	$ee_{(R)\text{-product}}$[a] [%]
1	*rac*-**1a**[b]	TOP-10	0.10	48.3	84.6	99.4	47	99.7
	rac-**1a**[b]	TOP-10	0.60	30.3	285.9	99.5		
2	*rac*-**1b**[b]	TDP-10	0.20	50.0	166.0	98.5	48	98.8
	rac-**1b**[b]	TDP-10	0.60	37.4	392.2	98.9		
3	*rac*-**3a**[c]	TOP-11	0.10	48.7	84.5	99.7	47	99.9
	rac-**3a**[c]	TOP-11	0.60	28.0	274.7	99.8		
4	*rac*-**3b**[c]	TDO-11	0.10	50.0	92.6	99.1	47	99.2
	rac-**3b**[c]	TDO-11	0.60	32.8	364.0	99.5		

[a] Analyzed by GC. [b] Acylating agent: vinyl acetate (2.76 equiv.) [c] Acylating agent: isopropyl 2-ethoxyacetate (0.6 equiv.)

7.4. Production of (R)-2a, (R)-4a by 30 h continuous-flow operation

The solution of the substrate (*rac*-**1a** or *rac*-**3a**, 48 mg mL^{-1}) and acylating agent (2.76 equiv. of vinyl acetate for *rac*-**1a** or 0.6 equiv. of isopropyl 2-ethoyxacetate for *rac*-**3a**) in dry toluene was pumped through the sol-gel immobilized *Ca*LB-filled columns (filling weights: 225.0 mg, **TDP**-10 *Ca*LB for *rac*-**1a**; 219.0 mg, **TDP**-11 *Ca*LB for *rac*-**3a**) thermostated at 60 °C at a flow rate of 0.1 mL min^{-1} for 30 h. In every 3 h, samples were collected (25 µL sample was diluted with ethanol to 975 µL) and analyzed (as described in Section 3.4 in ESI). After a series of experiments, columns were washed with toluene (0.5 mL min^{-1}, 30 min) and stored in refrigerator (4 °C).

8. Investigation of sol-gel entrapped CaLB by Raman spectroscopy

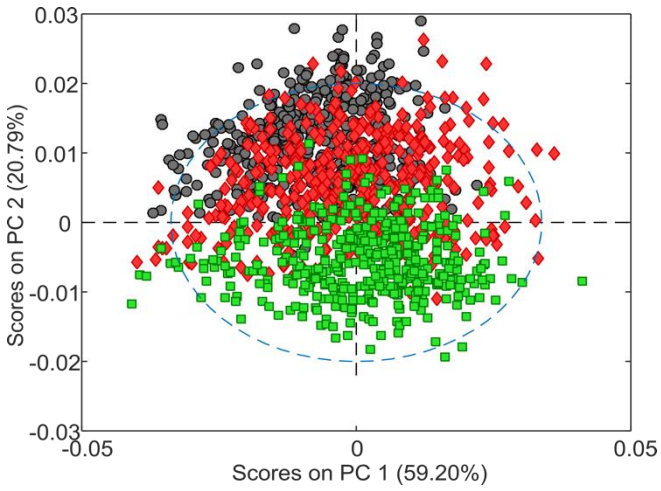

Fig.S12. Raman maps of sol-gel entrapped CaLB in TEOS/DMDEOS/PTEOS 10 systems at green dots) laboratory and grey dots) 100x large scale and red dots) enzyme free TEOS/DMDEOS/PTEOS sol-gel systems.

9. Particle size analysis of CaLB entrapped in sol-gel systems

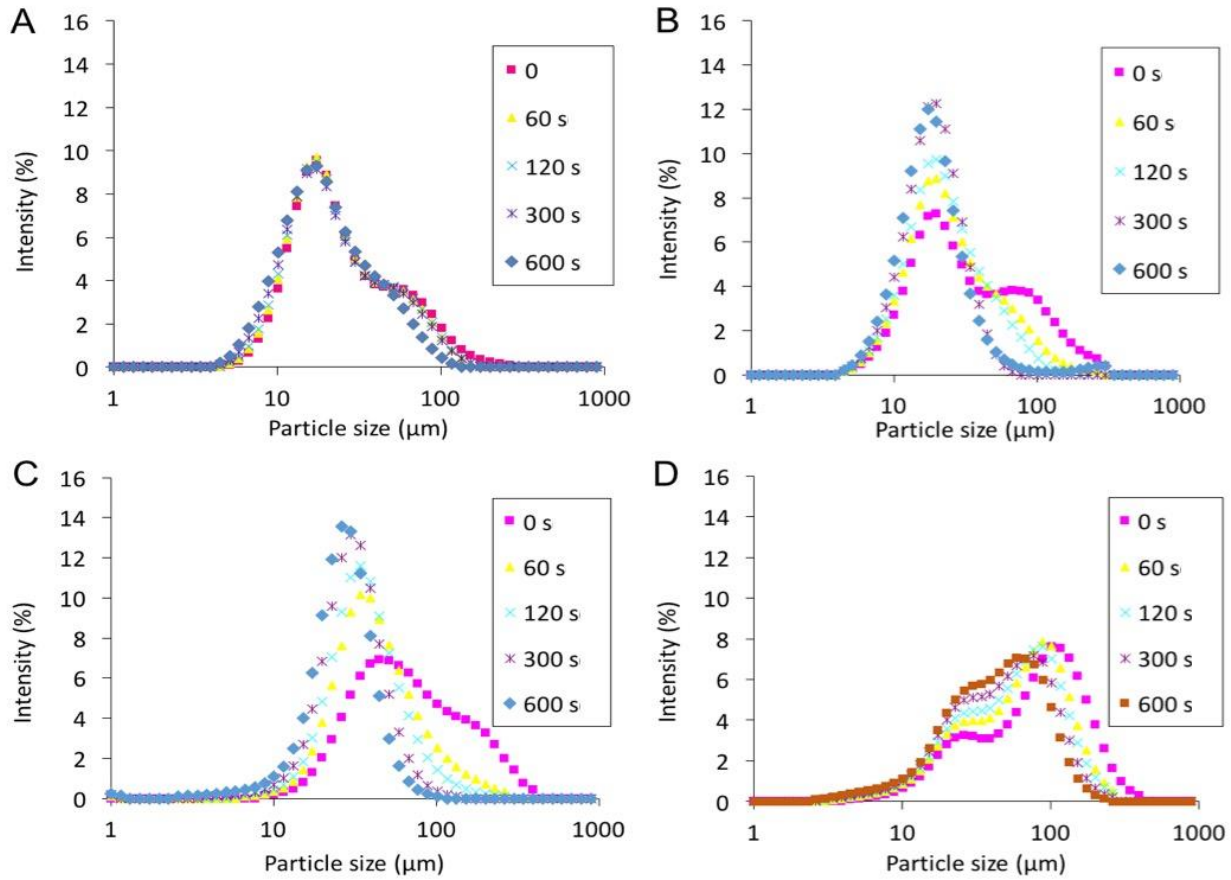

Fig. S13. Comparison of the particle size distribution of sol-gel entrapped CaLB. A) simple TEOS; B) binary TEOS/OTEOS; C) binary TEOS/PTEOS and D) ternary **TOP** systems.

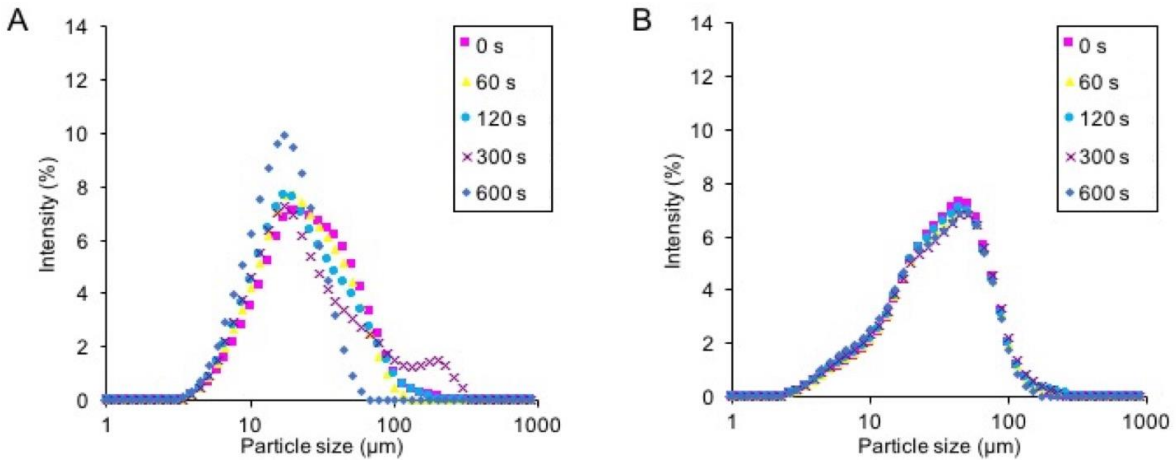

Fig. S14. Comparison of the particle size distribution of sol-gel entrapped CaLB in ternary **TDP**-10 system at A) laboratory and at B) 100x large scale.

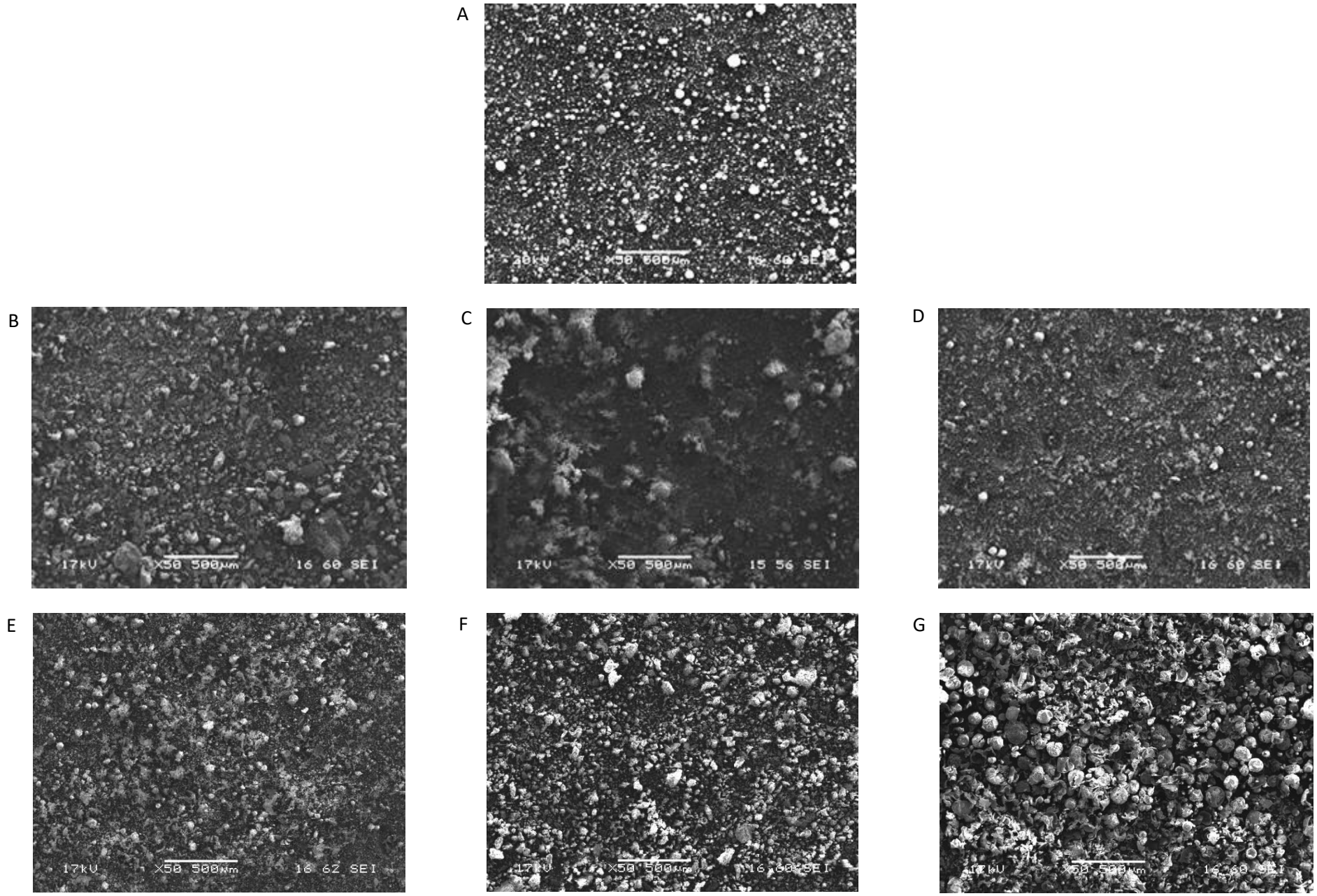

Fig S15. Scanning Electron Microscopic images of CaLB entrapped in sol-gel systems at magnification of 50×. A) TEOS, binary systems: B) TDP-4, C) TDP-5, D) TDO-5, ternary systems: E) TOP-10, F) TDP-10, G) TDO-10.

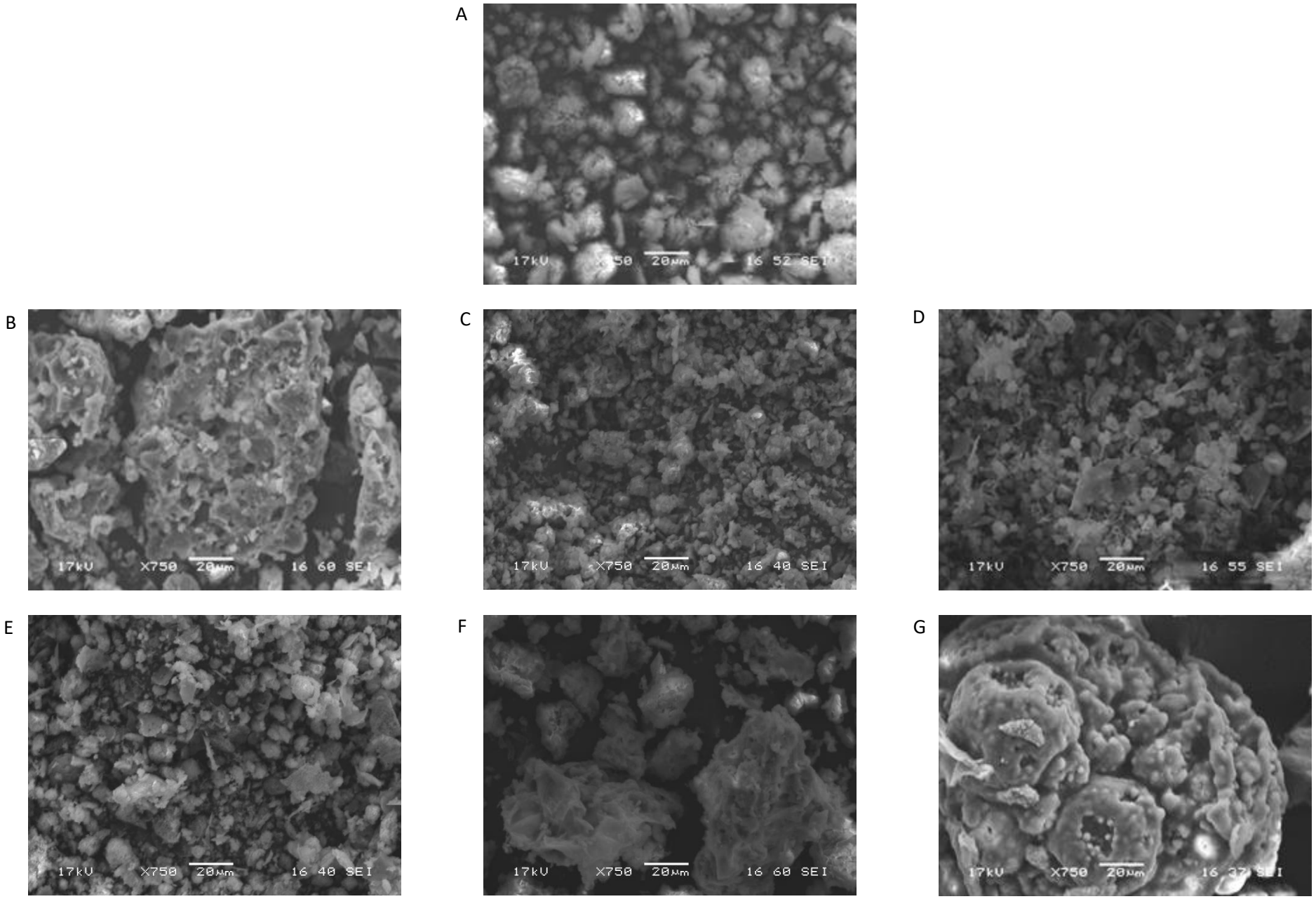

Fig S16. Scanning Electron Microscopic images of CaLB entrapped in sol-gel systems at magnification of 750×. A) TEOS, binary systems: B) TDP-4, C) TDP-5, D) TDO-5, ternary systems: E) TOP-10, F) TDP-10, G) TDO-10.

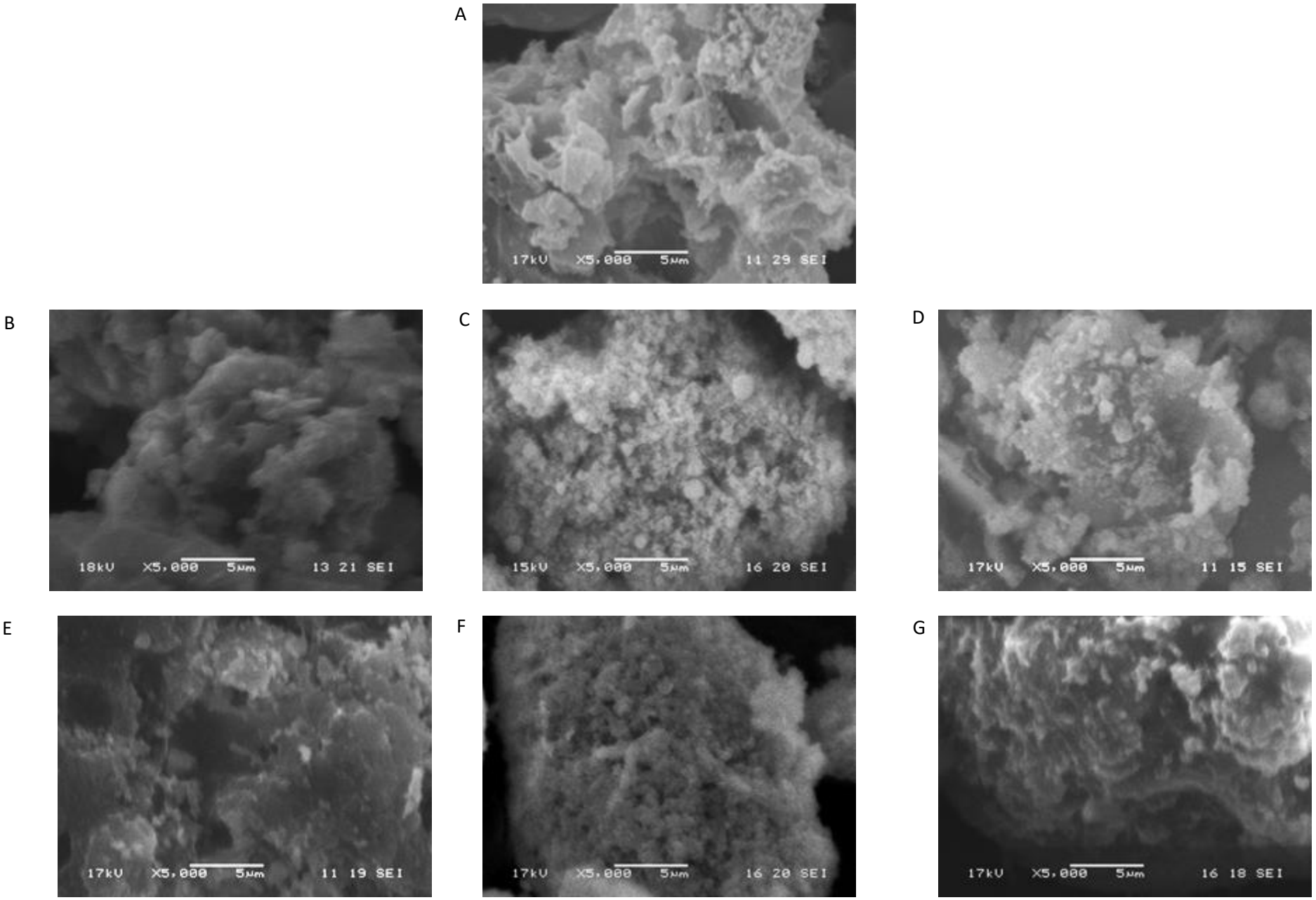

Fig S17. Scanning Electron Microscopic images of CaLB entrapped in sol-gel systems at magnification of 5000×. A) TEOS, binary systems: B) TDP-4, C) TDP-5, D) TDO-5, ternary systems: E) TOP-10, F) TDP-10, G) TDO-10.

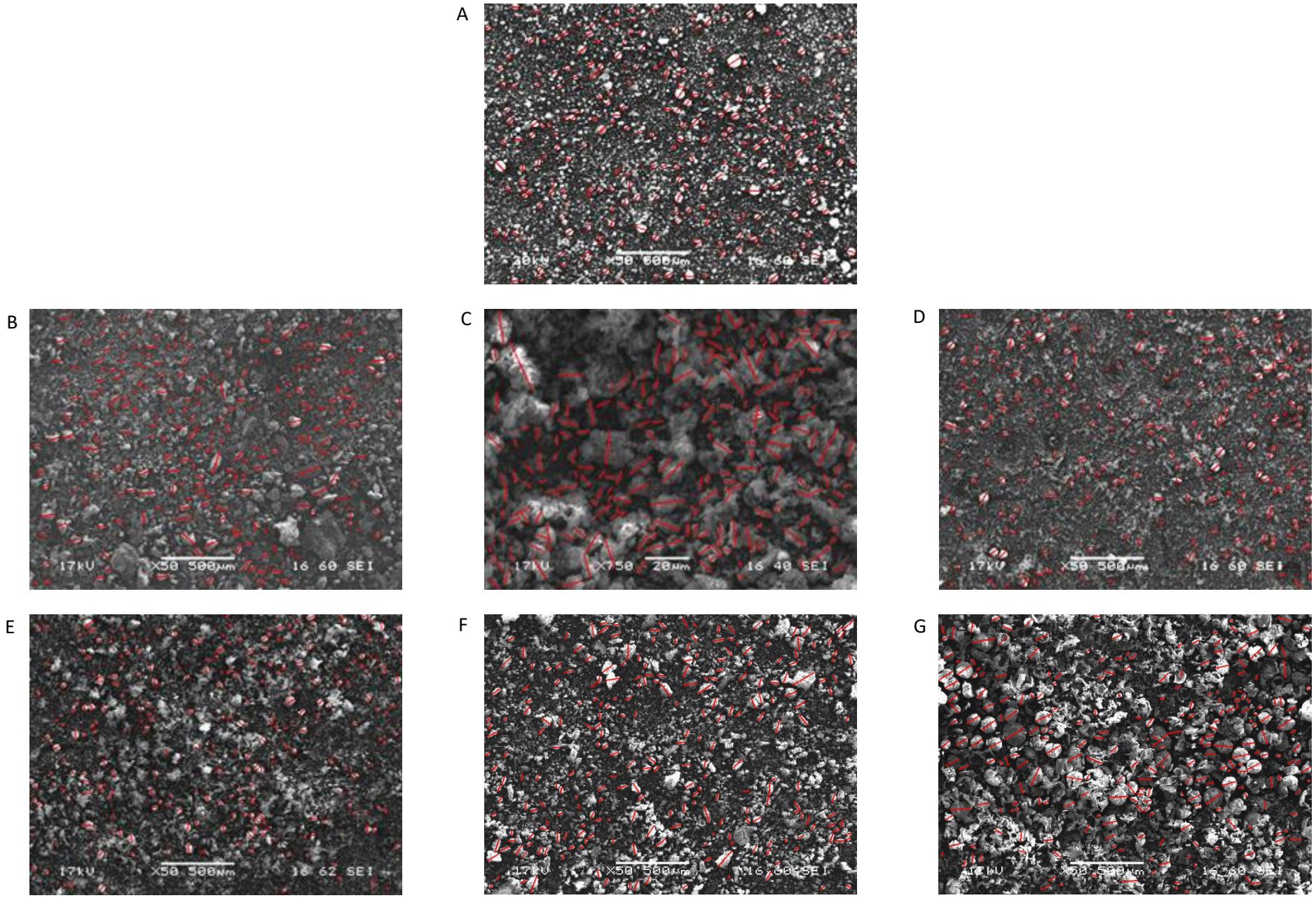

Fig S18. Scanning Electron Microscopic images of CaLB entrapped in sol-gel systems for particle size distribution analysis at magnification of 50× (except for C) TP-5 at magnification of 750×). A) TEOS; binary systems: B) TDP-4, C) TDP-5 (750×), D) TDO-5; ternary systems: E) TOP-10, F) TDP-10, G) TDO-10. Red lines are the markers for particle diameters.

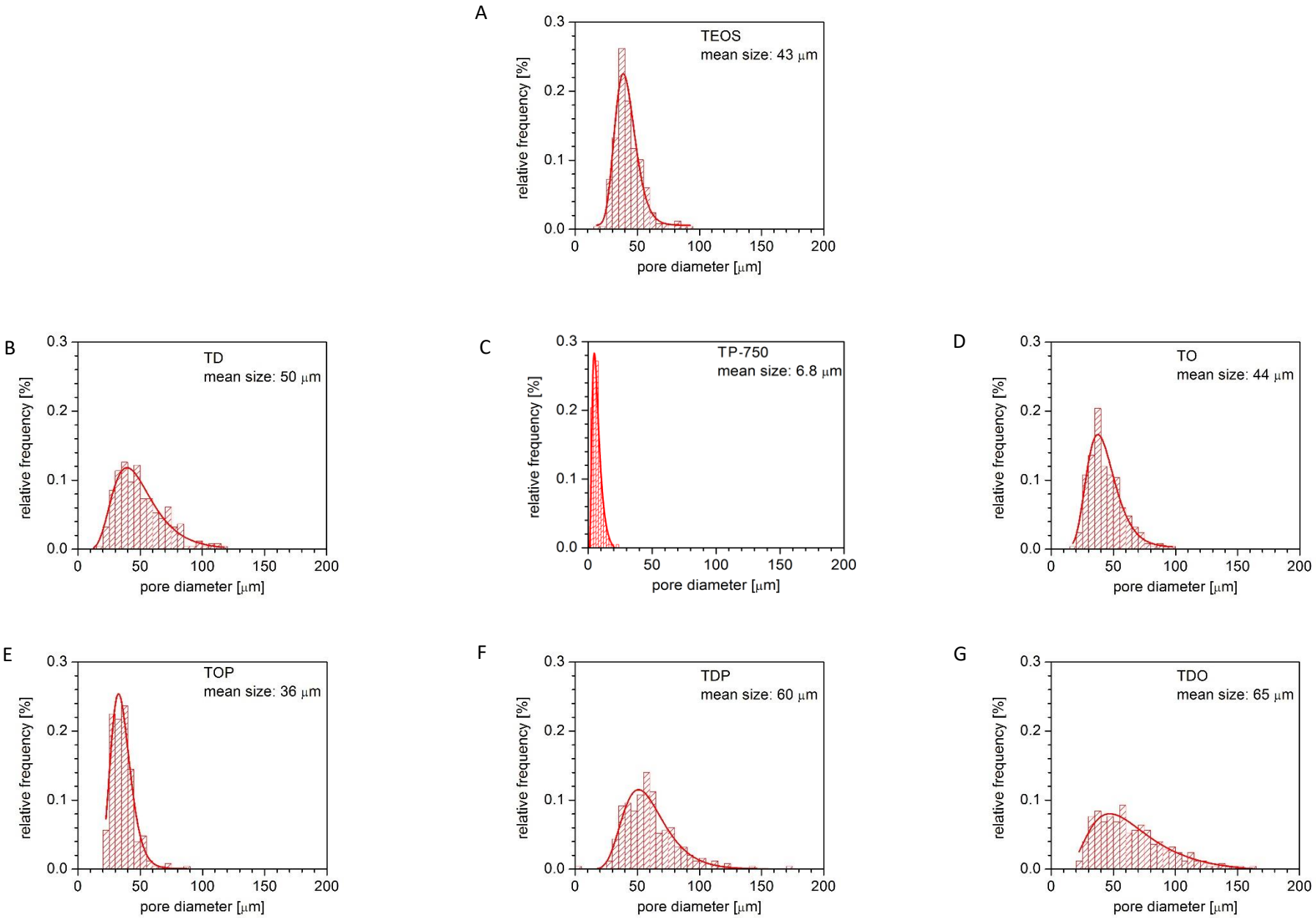

Fig S19. Particle size distribution of sol-gel entrapped CaLB biocatalysts determined by analysis of SEM images. A) TEOS, binary systems: B) TDP-4, C) TDP-5, D) TDO-5, ternary systems: E) TOP-10, F) TDP-10, G) TDO-10.

10. Morphology and biocatalytic activity of CaLB entrapped in selected sol-gel systems

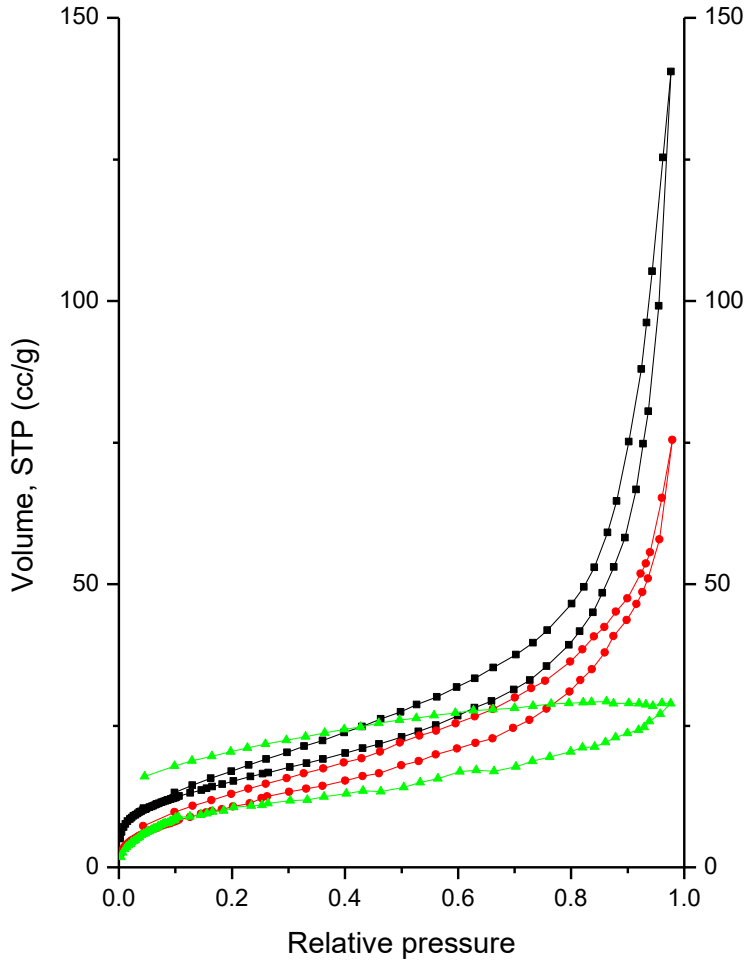

Fig S20. Representative isotherms from nitrogen adsarption/desorption analysis of different sol-gel entrapped CaLB biocatalysts: ■TEOS (TDP-1), ◆TEOS/PTEOSP (TDP-5), ▲ TEOS/DMDEOS/PTEOS (TDP-10).

Table S11. Specific surface, porosity and particle size characteristics of the CaLB immobilized sol-gel materials with biocatalytic properties

Sol-gel entrapped CaLB biocatalyts	Specific surface area ($m^2\ g^{-1}$)	Total volume of pores (2-50 nm) ($cm^3\ g^{-1}$)	Volume of nanopores (<2 nm) ($cm^3\ g^{-1}$)	Density ($g\ cm^{-3}$)	Main particle size according to SEM (μm)	Main particle size according to Mie scattering (μm)	r_{batch} ($U\ g^{-1}$)
TEOS (TDP-1)[a]	57	0.22	0.02	1.80	43	28	16.5
TEOS/PETOS (TDP-5)[b]	46	0.09	0.01	1.44	7	53	47.0
TEOS/DMDEOS/PTEOS (TDP-10)[c]	40	0.05	0.01	1.49	60	64	67.4

[a] Simple TEOS precursor system, see in Table S2. point 1, [b] binary precursor system by TEOS/PTEOS=0.413/0.586 (see in Table S2, point 5),
[c] ternary precursor system by TEOS/DMDEOS/PTEOS=0.413/0.293/0.293 (seen in Table S2. point 10)

Table S12. Specific surface and porosity characteristics of the sol-gel materials without CaLB

Sol-gel systems	Specific surface area ($m^2\ g^{-1}$)	Total volume of pores ($cm^3\ g^{-1}$)	Density ($g\ cm^{-3}$)
TEOS (TDP-1)[a]	101	0.30	1.79
TEOS/PETOS (TDP-5)[b]	5	0.02	1.23
TEOS/DMDEOS/PTEOS (TDP-10)[c]	166	0.30	1.62

[a] Simple TEOS precursor system, see in Table S2. point 1, [b] binary precursor system by TEOS/PTEOS=0.413/0.586 (see in Table S2, point 5),
[c] ternary precursor system by TEOS/DMDEOS/PTEOS=0.413/0.293/0.293 (seen in Table S2, point 10)

11. FT-IR analysis of CaLB entrapped in selected sol-gel systems

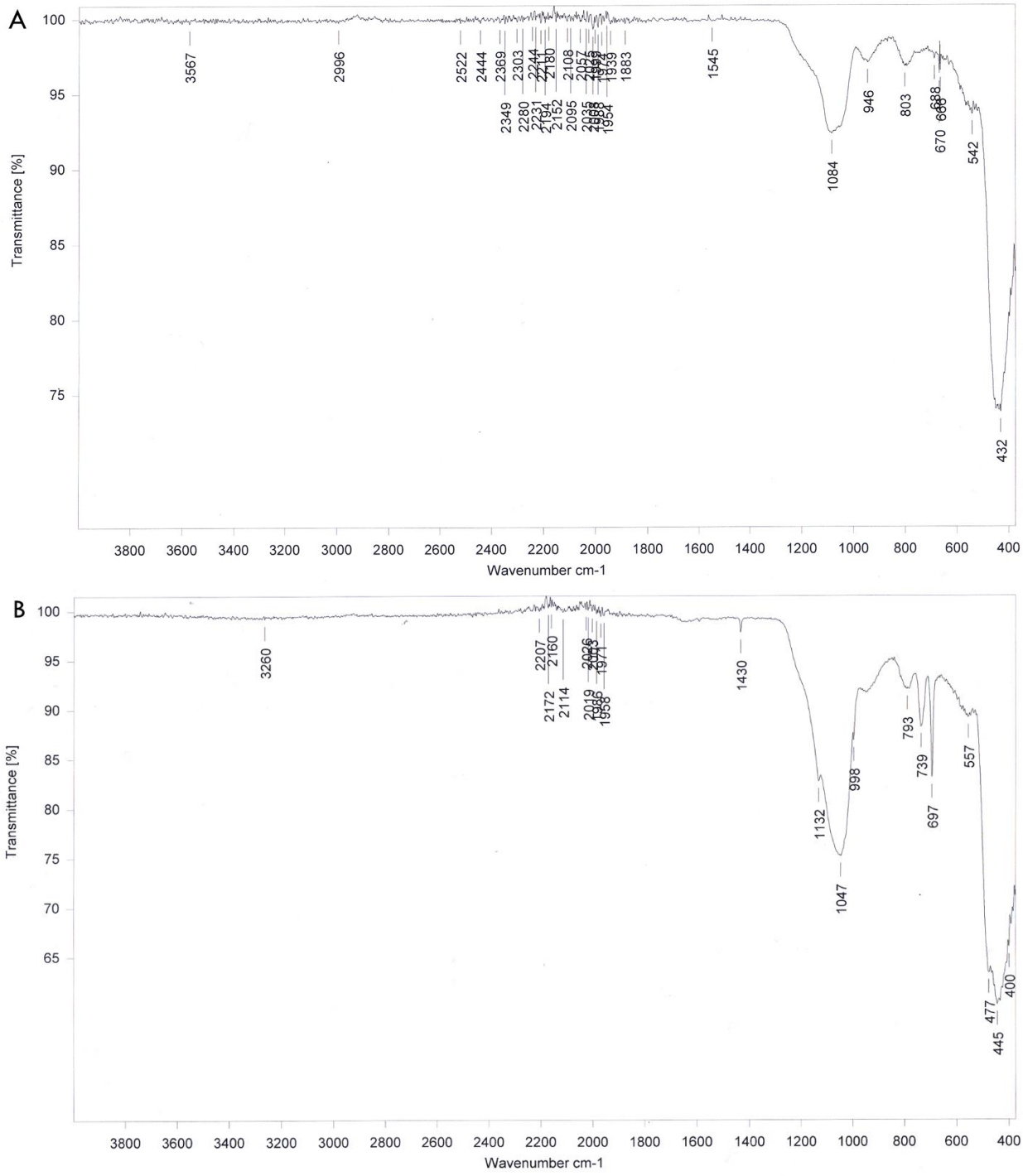

Fig S20. FT-IR spectra of sol-gel entrapped CaLB biocatalysts (ATR mode). A) Simple TEOS precursor system, see in Table S2. point 1, B) TDP-4 binary precursor system by TEOS/DMDEOS=0.413/0.586 (see in Table S2. point 4)

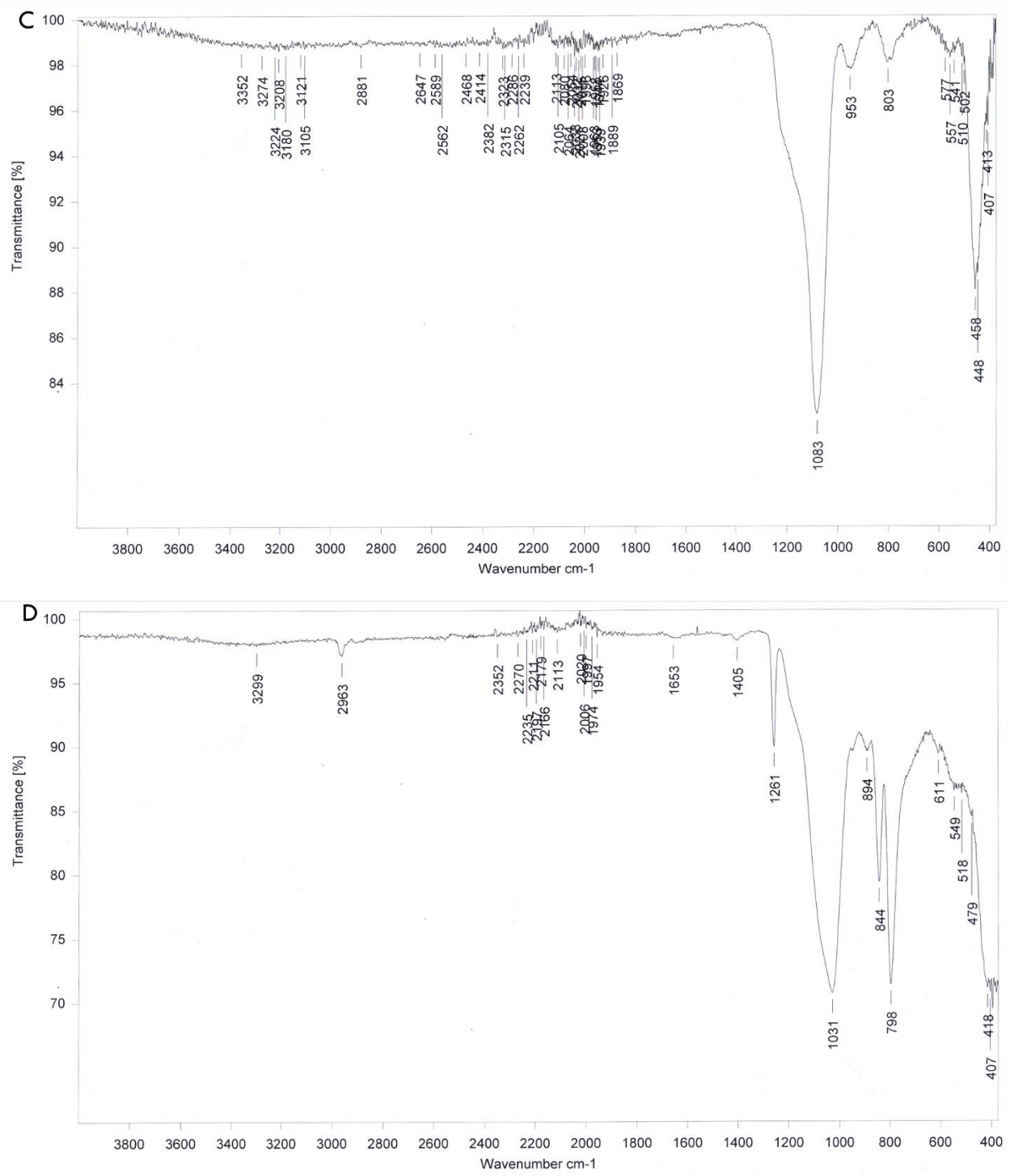

Fig S21. FT-IR spectra of sol-gel entrapped CaLB biocatalysts (ATR mode). C) TDP-5 binary precursor system by TEOS/PTEOS=0.413/0.586 (see in Table S2. point 5) and D) TDO-5 binary precursor system by TEOS/OTEOS=0.413/0.586 (see in Table S2. point 5)

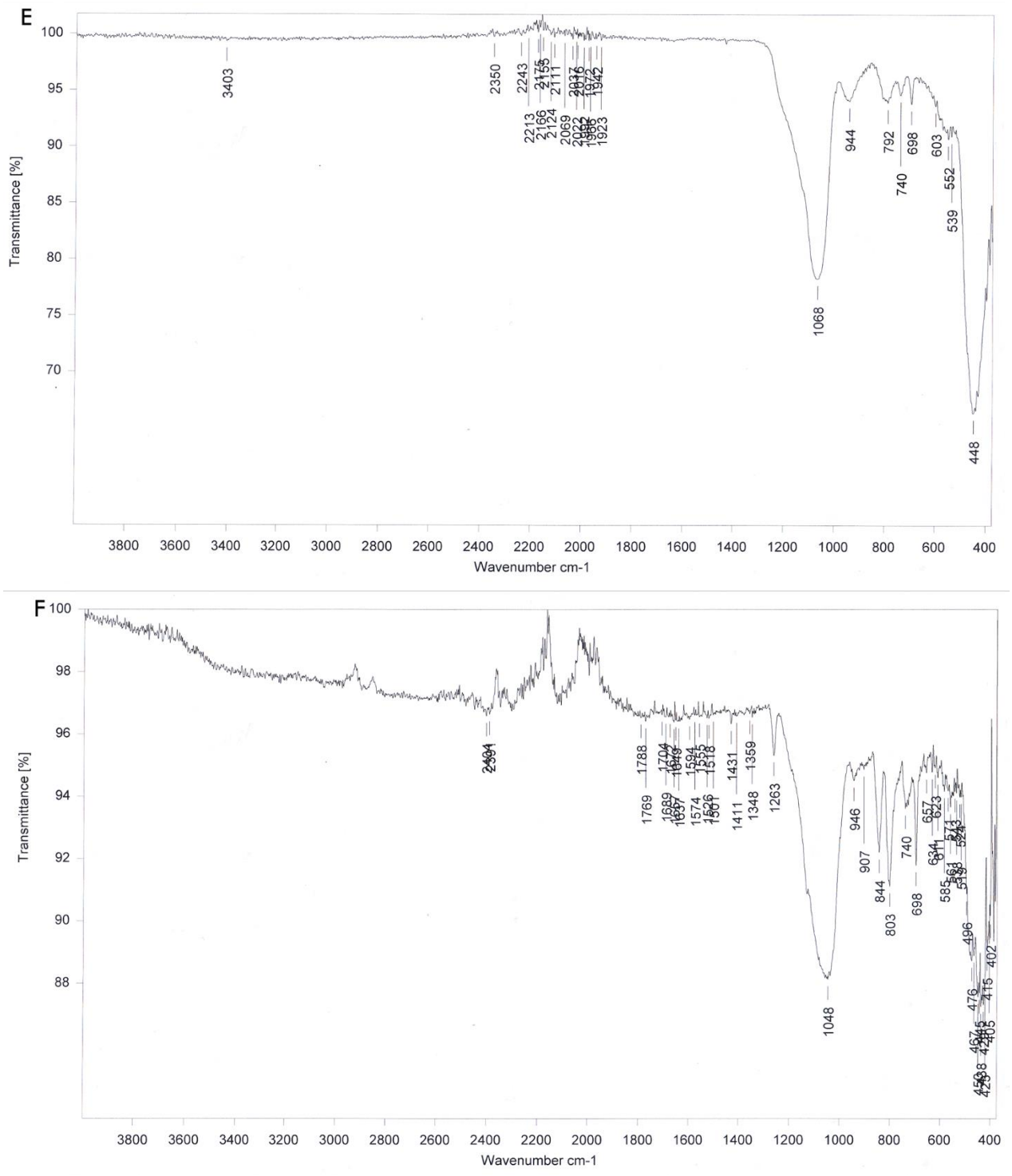

Fig S22. FT-IR spectra of sol-gel entrapped CaLB biocatalysts (ATR mode). E) TOP-10 ternary precursor system by TEOS/OTEOS/PTEOS=0.413/0.293/0.293 (seen in Table S2. point 10) and F) TDP-10 ternary precursor system by TEOS/DMDEOS/PTEOS=0.413/0.293/0.293 (seen in Table S2. point 10)

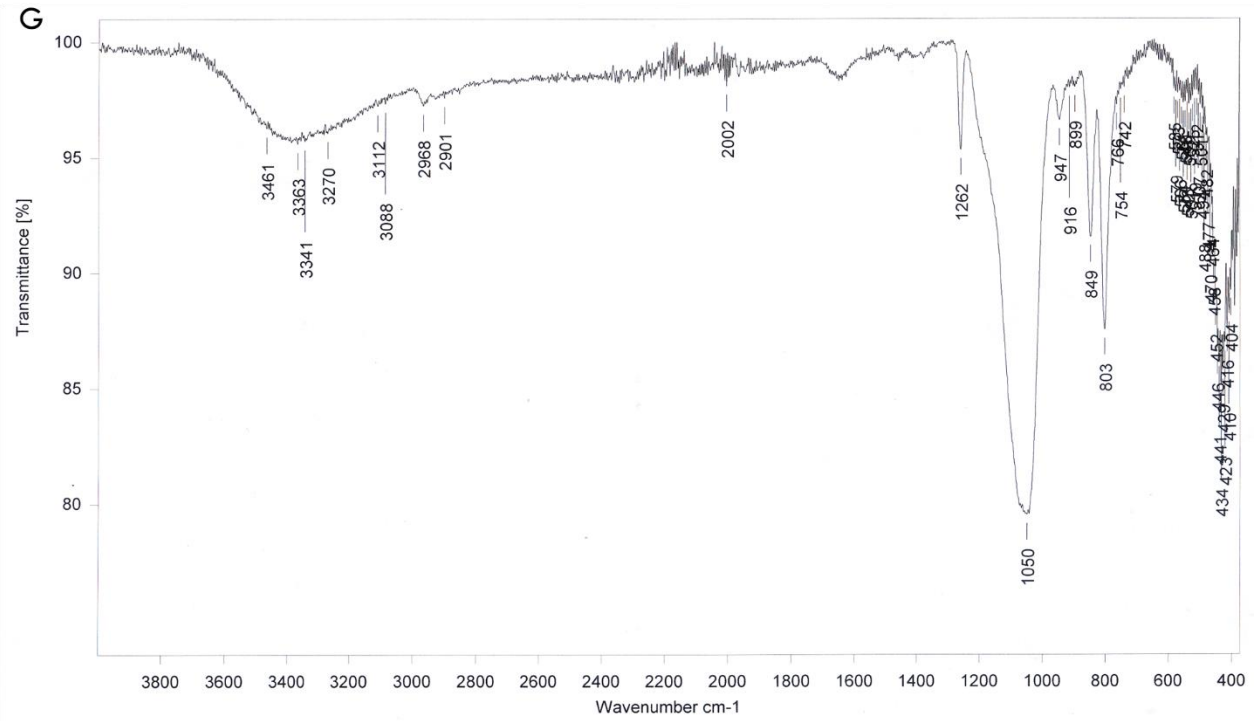

Fig S23. FT-IR spectra of sol-gel entrapped CaLB biocatalysts (ATR mode). G) TDO-10 ternary precursor system by TEOS/DMDEOS/OTEOS=0.413/0.293/0.293 (seen in Table S2. point 10)

References

1 M. Oláh, Z. Boros, G. Hornyánszky, L. Poppe, *Tetrahedron,* 2016, **72**, 7249–7255.

2 R. G. Newton, In *Scattering Theory of Waves and Particles (2nd Edition)*. Springer. New York. 1982, pp. 48–50.

3 S. Brunauer, P. Emmett, E. Teller, *J. Am. Chem. Soc.,* 1938, **60**, 309–319.

4 M. M. Dubinin, L. V. Radushkevich, *Proc. Acad. Sci. USSR. Phys. Chem. Sect.,* 1947, **55**, 331–337.

5 J. Yuan, N. Han, H. Yi, Y. Wang, S. Yang, J. C. Wong, WO2014145512 A3, 2014.

6 C. S. Chen, Y. Fujimoto, G. Girdaukas, J. Sih, *J. Am. Chem. Soc*., 1982, **104**, 7294–7299.

7 C. Csajági, G. Szatzker, E. R. Tőke, L. Ürge, F. Darvas, L. Poppe, *Tetrahedron:Asymmetry*. 2008, **19**, 237–246.

8 (a) Protein Preparation Wizard 2015-4; Epik version 2.4, Schrödinger, LLC, New York, NY, 2015; Impact version 5.9, Schrödinger, LLC, New York, NY, 2015; Prime version 3.2, Schrödinger, LLC, New York, NY, 2015. (b) G. M. Sastry, M. Adzhigirey, T. Day, R. Annabhimoju, W. J. Sherman, Comput. Aid. Mol. Des., 2013, **27**, 221-234.

9 D. Weiser, P. L. Sóti, G. Bánóczi, V. Bódai, B. Kiss, Á. Gellért, Zs. K. Nagy, B. Koczka, A. Szilágyi, Gy. Marosi, L. Poppe, *Tetrahedron*, 2016, **72**, 7335–7342.

10 (a) Glide, Schrödinger, LLC, New York, NY, USA, 2015; (b) R. A. Friesner, J. L. Banks, R. B. Murphy, T. A. Halgren, J. J. Klicic, D. T. Mainz, M. P. Repasky, E. H. Knoll, D. E. Shaw, M. Shelley, J.K. Perry, P. Francis, P. S. Shenkin, *J. Med. Chem*., 2004, **47**, 1739-1749; (c) R. A. Friesner, R. B. Murphy, M. P. Repasky, L. L. Frye, J. R. Greenwood, T. A. Halgren, P. C. Sanschagrin, D. T. Mainz, *J. Med. Chem*., 2006, **49**, 6177-6196; (d) T. A. Halgren, R. B. Murphy, R. A. Friesner, H. S. Beard, L. L. Frye, W. T. Pollard, J. L. Banks, *J. Med. Chem*., 2004, **47**, 1750–1759.

11 Prime, version 4.2, Schrödinger, LLC, New York, NY, USA, 2015.

12 MacroModel, version 11.0, Schrödinger, LLC, New York, NY, USA, 2015

13 Statistica 12 (http://www.statsoft.com/Products/STATISTICA-Features/Version-12, retrieved 20. 07. 2016.)